Journal of Mathematical Modeling
Vol. -, No. -, 2026, pp. -. Research Article

JMM

A two-stage robust–probabilistic method for an adaptive relief logistics network with perishable products under uncertainty

Seyed Sina Miri-Nargesi[a], Salman Nazari-Shirkouhi[b]*, Seyyed Mohammad Hadji Molana[a], Reza Tavakkoli-Moghaddam[c,d]

[a] *Department of Industrial Engineering, SR.C., Islamic Azad University, Tehran, Iran*
[b] *Department of Industrial and Systems Engineering, Fouman Faculty of Engineering, College of Engineering, University of Tehran, Tehran, Iran.*
[c] *School of Industrial Engineering, College of Engineering, University of Tehran, Tehran, Iran//*
[d] *Research Center of Performance and Productivity Analysis, Istinye University, Istanbul, Turkey*

Email(s): s.mirinargesy@iau.ac.ir, snnazari@ut.ac.ir, molana@iau.ac.ir, tavakoli@ut.ac.ir

Abstract. Natural disasters challenge relief logistics due to demand uncertainty, limited supply, and the perishability of relief items. This study develops a bi-objective crisis logistics network model that integrates shelf-life constraints, public aid flows, and demand–supply uncertainty within a two-stage robust-probabilistic framework. The model jointly determines permanent and temporary aid-base locations, perishable item allocation, inventory decisions, and public aid distribution. An enhanced ε-constraint method is used to generate Pareto-efficient solutions. A real case study of Tehran shows that the first efficient solution selects three permanent and seven temporary aid bases, with a total cost of USD 953,811.99 and maximum unmet demand of 1,536.24 kg. Moving toward service-oriented solutions reduces unmet demand by about 47.7%. Robustness analysis shows that increasing the uncertainty-control level from 0.5 to 0.9 raises total cost by 5.10% and unmet demand by 38.98%. Scalability and benchmark analyses further confirm the applicability and balanced performance of the proposed framework for urban disaster-response planning.

Keywords: Crisis logistics network, disaster management, two-stage robust-probabilistic model, perishable items.
AMS Subject Classification 2010: 90B06, 90B80, 90C11, 90C29, 90C90

1 Introduction

In recent decades, natural disasters have caused extensive damage to urban infrastructure and resulted in substantial human and economic losses worldwide. Densely populated urban areas are particularly

*Corresponding author

Received: 25 April 2026/ Revised: 29 August 2026/ Accepted: 02 September 2026
DOI: 10.22124/jmm.2026.33354.3049

vulnerable to such events; since the early twentieth century, more than 22,000 natural disasters have been recorded globally, leading to over eight million fatalities [21]. Iran is consistently ranked among the ten most disaster-prone countries and is frequently exposed to earthquakes, floods, and other large-scale crises, often accompanied by severe casualties and significant economic disruption. Despite increasing scientific and managerial attention, the occurrence, magnitude, and impacts of natural disasters remain largely unpredictable and uncontrollable, limiting the effectiveness of purely preventive strategies [5].

Given this inherent uncertainty, timely and well-coordinated response actions are essential to mitigating both human suffering and economic damage. The growing scale and complexity of modern disasters necessitate integrated and efficient supply chain planning to ensure the rapid delivery of essential relief items. Under such conditions, relief management and humanitarian logistics systems are primarily driven by social objectives, including saving lives, reducing shortages, and minimizing operational costs. Consequently, the effectiveness of post-disaster response depends not only on resource availability but also on the structural design and operational efficiency of the logistics network.

In conventional supply chain planning, multiple stakeholders, such as suppliers, manufacturers, and distributors, coordinate to ensure the smooth flow of goods. In disaster contexts, however, supply chain performance becomes substantially more critical, as it directly influences survival rates and the overall success of relief operations during events such as earthquakes and floods. Disaster management systems typically consist of three interconnected subsystems: command, operations, and logistics, with logistics serving as the backbone of crisis response. Humanitarian logistics encompasses activities related to the estimation, procurement, transportation, storage, and distribution of relief supplies and services for disaster victims and response teams. These activities span multiple operational phases, including pre-disaster preparedness, emergency response, and post-disaster recovery, each requiring rapid decision-making under severe time and resource constraints [9].

Recent studies increasingly emphasize the integration of advanced technologies with humanitarian logistics to enhance adaptability and responsiveness. AI-based routing systems, real-time inventory management, machine learning techniques, and demand forecasting methods have been shown to improve coordination and decision-making in dynamic crisis environments, particularly for managing perishable relief items [11]. In parallel, fuzzy–probabilistic modeling and reinforcement learning approaches, such as Proximal Policy Optimization, have demonstrated strong potential for handling uncertainty in humanitarian supply chains [16]. However, despite these methodological advances, most existing studies address uncertainty and perishability as separate challenges, resulting in fragmented decision-making frameworks that fail to capture their joint impact in resource-constrained crisis settings.

Given the increasing frequency and severity of natural disasters, crisis logistics systems must support timely relief distribution under uncertain demand and supply conditions. This challenge is more critical for perishable relief items, whose usability may rapidly decline due to delays in storage, allocation, or delivery. Therefore, emergency planners need a structured framework for locating aid bases, allocating perishable supplies, managing public aid flows, and addressing uncertainty. This study develops a bi-objective crisis logistics network design model for perishable relief items under uncertainty. The model determines the locations of permanent and temporary aid bases, allocates perishable items to affected areas, manages public and celebrity aid flows, and controls inventory and shipment decisions subject to shelf-life limitations. Accordingly, this study addresses the following research questions:

1. How should permanent and temporary aid bases be jointly located under uncertain disaster conditions?

2. How should perishable relief items be allocated and stored while respecting shelf-life constraints?
3. How can public and celebrity aid flows be incorporated into the relief network?
4. How can demand and supply uncertainty be incorporated into the model to evaluate the trade-off between total logistics cost and maximum unmet demand?

To answer these questions, a two-stage robust–probabilistic optimization model is developed. The bi-objective model is solved using the enhanced ε-constraint method, and its applicability is demonstrated through a real-world case study of Tehran's metropolitan area.

The remainder of this paper is organized as follows. Section 2 reviews the relevant literature on crisis logistics, humanitarian supply chains, and uncertainty-aware network design. Section 3 presents the problem description and develops the proposed bi-objective robust–probabilistic crisis logistics model. Section 4 describes the solution methodology based on the enhanced ε-constraint approach. Section 5 reports the case study and numerical results, including sensitivity analyses. Finally, Section 7 concludes the paper and outlines managerial implications and directions for future research.

2 Literature review

Humanitarian logistics and crisis supply chain management constitute a mature yet continuously expanding research domain, motivated by the increasing frequency and severity of disasters. Although the literature addresses a wide range of topics, this study adopts a focused and analytical perspective. Accordingly, the review concentrates on two interrelated streams that are most directly aligned with the objectives of the present work: (i) humanitarian logistics network design and (ii) uncertainty modeling in crisis logistics.

2.1 Humanitarian logistics network models

Humanitarian logistics network design has been widely recognized as a fundamental decision layer for disaster preparedness and response. Vahdani et al. [16] proposed a two-phase, multi-period, and multi-commodity mixed-integer model that jointly optimized relief facility location and material allocation under uncertainty. Their study showed that separating strategic location decisions from tactical allocation decisions could lead to inefficient network configurations, particularly when multiple humanitarian objectives are considered. Nayeem and Lee [8] further highlighted the vulnerability of deterministic network designs by showing that ignoring demand uncertainty could significantly degrade system performance, even when facility locations are optimally selected.

Recent decision-support studies have also emphasized the importance of prioritization in relief operations. Shadkam and Cheraghchi [14] developed a hybrid two-phase approach for prioritizing earthquake-affected regions and dispatching relief teams by combining AHP, TOPSIS, AHP–TOPSIS, and CoCoSo. Their study contributed to post-earthquake prioritization; however, it focuses on ranking affected regions rather than designing an integrated relief logistics network under uncertainty.

To address operational interdependencies, Aliakbari et al. [2] demonstrated that travel-time uncertainty and multi-period routing flexibility substantially affected service levels in large-scale disaster environments. Mahtab et al. [6] showed that incorporating temporary relief bases across preparedness and response phases can enhance network adaptability. Consistent with this stream, Vahdani et al. [16]

emphasized that two-stage location–inventory decisions under uncertainty could improve humanitarian network responsiveness, while Aliakbari et al. [2] showed that cross-docking structures can strengthen strategic–operational coordination. Related transportation-oriented optimization studies also emphasized the importance of integrating allocation and transportation decisions. Ziaee et al. [22] developed a multi-agent optimization model with explicit transportation constraints and highlighted the importance of transportation cost and timely delivery in geographically distributed systems. Related supply-chain research has also explicitly considered perishability together with reliability and disruption in network design [4], although that work is not specific to humanitarian relief logistics. Overall, these studies confirm that humanitarian logistics performance depends on the joint design of facility location, allocation, inventory, and distribution decisions under uncertainty. However, most existing network models treat relief commodities as homogeneous and time-insensitive, and public aid flows are rarely modeled as endogenous network flows. Moreover, although temporary facilities have been considered in some studies, their coordination with permanent aid bases under perishability and simultaneous demand–supply uncertainty remains insufficiently explored. Therefore, further integration is needed between network design, facility flexibility, public aid management, and perishability-aware allocation decisions.

2.2 Uncertainty modeling in crisis logistics optimization

Uncertainty is a defining feature of disaster environments, affecting demand, supply availability, travel conditions, facility reliability, and the timing of relief operations. Accordingly, a large body of research has attempted to incorporate uncertainty into humanitarian logistics models. Boostani et al. [3] showed that considering demand and supply uncertainty in multi-objective humanitarian logistics could lead to substantially different cost, coverage, and sustainability outcomes compared with deterministic models. Modiri et al. [7] adopted a robust fuzzy optimization framework to address economic, social, and environmental objectives under uncertainty, while Seraji et al. [13] developed a two-stage multi-objective model that incorporated distributive injustice and dissatisfaction. These studies were important because they moved beyond cost-oriented planning and showed that uncertainty also affected social and humanitarian performance. However, their treatment of relief commodities is relatively general, and the operational consequences of perishability are not fully embedded in the uncertainty structure.

Recent studies have further shifted attention toward reliability, disruption resilience, and healthcare-related emergency supply chains. Wang et al. [18] applied global robust optimization to casualty transportation and medical equipment distribution. Abbasi et al. [1] incorporated facility failure and pandemic-related disruptions into uncertainty-aware network design. In a related healthcare context, Rajabi et al. [10] proposed a bi-objective pharmaceutical supply chain network under COVID-19 disruption to minimize costs and shortages, considering temporary distribution points and backup inventory. These studies improved the modeling of disrupted supply systems and highlighted the importance of backup capacity and resilient facility planning. Nevertheless, most of them focus on general healthcare or relief supply chains and do not explicitly capture the interaction among perishability, public aid inflows, and permanent–temporary aid-base coordination.

More recent distributionally robust optimization studies have strengthened the state of the art by addressing ambiguity in probability distributions and incomplete disaster information. Zhang et al. [19] developed a two-stage DRO model for humanitarian transportation network design by jointly optimizing road-link strengthening, inventory pre-positioning, and post-disaster transportation. Wang et al. [17] proposed a distributionally robust chance-constrained model for multi-period emergency resource allocation and vehicle routing under demand ambiguity and dynamic disaster risk. Similarly, Sarmadi and Amiri-Aref [12] formulated a joint chance-constrained DRO approach for multi-period location-routing in urban search-and-rescue operations under uncertain demand and travel times. Zhang et al. [20] further integrated emergency facility location, inventory pre-positioning, and evacuation planning within a two-stage DRO framework. These studies provided strong methodological advances, particularly in modeling ambiguity, dynamic response, routing, evacuation, and infrastructure reliability. However, their emphasis is mainly on general relief resources, evacuation flows, vehicle routing, or infrastructure disruption, while shelf-life-dependent perishability and public aid flows are usually outside the core modeling structure.

From a methodological perspective, Shadkam et al. [15] proposed a hybrid COA/ε-constraint approach for multi-objective supplier selection and showed its effectiveness in generating Pareto solutions. Although their study is not directly focused on humanitarian logistics, it supported the relevance of ε-constraint-based approaches for solving complex multi-objective optimization problems.

Overall, the reviewed uncertainty-aware studies have significantly improved the robustness and reliability of humanitarian logistics planning. However, they often addressed uncertainty, perishability, facility flexibility, and aid-flow management as separate modeling concerns. This indicates a need for integrated formulations that jointly capture demand–supply uncertainty, shelf-life-dependent relief items, public aid flows, and permanent–temporary aid-base coordination within a single crisis logistics network design model.

2.3 Gap analysis

Taken together, the reviewed literature shows substantial progress in humanitarian logistics network design, perishability-aware relief distribution, and uncertainty modeling through stochastic, robust, fuzzy, and distributionally robust optimization approaches. However, these research streams have often been developed separately, and their integration within a single crisis logistics network design model remains limited. In particular, existing studies have widely examined facility location and relief allocation under uncertainty, but fewer models simultaneously consider perishable relief items, permanent and temporary aid bases, public aid inflows, and joint demand–supply uncertainty within the same bi-objective optimization framework.

More specifically, three main research gaps can be identified. First, although uncertainty has been extensively studied in humanitarian logistics, many existing models either assume relief items to be non-perishable or treat perishability mainly as an operational distribution issue. This limits their ability to capture how shelf-life restrictions affect facility selection, allocation decisions, inventory feasibility, and unmet demand under uncertain disaster conditions. In crisis logistics, this interaction is important because delayed or poorly allocated shipments may become unusable before reaching affected areas.

Second, previous studies have often addressed permanent and temporary relief facilities separately. Permanent facilities are generally associated with pre-disaster preparedness, while temporary facilities are usually considered as flexible response resources after a disaster occurs. However, fewer studies coordinate these two types of facilities within a unified location–allocation structure. This separation restricts the ability of existing models to evaluate the trade-off between stable pre-disaster capacity and flexible post-disaster response capacity, particularly when relief items are perishable and demand conditions are uncertain.

Third, public and spontaneous aid flows are often simplified or treated as external resources in optimization-based humanitarian logistics models. In practice, public and celebrity donations may constitute an important source of relief supply, but they must be properly directed to permanent bases, temporary bases, or affected areas to avoid inefficient allocation and operational imbalance. Therefore, incorporating such aid flows as explicit network flows can improve the realism of crisis logistics modeling.

Accordingly, the research gap addressed in this study is not the general absence of uncertainty modeling, facility location, or perishability considerations in humanitarian logistics, since each of these topics has already been investigated in prior research. Rather, the specific gap lies in the limited integration of these elements within a single model: age-sensitive perishability constraints, permanent–temporary aid base coordination, public aid flows, and simultaneous demand–supply uncertainty, while balancing total logistics cost and maximum unmet demand. These identified gaps provide the basis for clarifying the theoretical and practical novelty of the present study in the following section.

2.4 Theoretical and practical novelty of the study

Based on the comparative evidence presented in Table 1, prior studies differ not only in their decision scope but also in the way they represent uncertainty and operational realism in humanitarian logistics. Stochastic and scenario-based models are useful for representing alternative disaster conditions, but they may provide limited protection against unfavorable deviations within each scenario. In contrast, robust and distributionally robust models improve protection against uncertainty, although they may lead to conservative solutions or require additional ambiguity-set assumptions. This distinction is particularly important in crisis logistics, where both the likelihood of disaster scenarios and the severity of demand and supply deviations should be reflected in the planning model.

In this regard, the proposed robust–probabilistic framework is positioned as a problem-specific compromise between purely probabilistic and purely robust formulations. Scenario probabilities capture the relative likelihood of disaster scenarios in the objective functions, whereas the robustness-control parameters regulate adverse within-scenario deviations in demand, permanent-base supply, and public aid availability, respectively. Therefore, the probabilistic and robust components play complementary roles: the former evaluates expected system performance across scenarios, while the latter protects the network against higher-than-expected demand and lower-than-expected supply within each scenario.

The novelty of this study should not be interpreted as the introduction of a completely new optimization paradigm. Rather, its contribution lies in the problem-driven integration of several modeling elements that are commonly treated separately in the humanitarian logistics literature. The bi-objective structure captures the cost–shortage trade-off, while the two-stage robust–probabilistic formulation links strategic facility-location decisions with scenario-dependent allocation, inventory, and shipment decisions under simultaneous demand and supply uncertainty. In addition, the perishability mechanism connects product shelf life with inventory and shipment feasibility, enabling the model to capture the operational consequences of delayed or inefficient distribution of time-sensitive relief items.

From a practical perspective, the proposed framework reflects key features of real crisis logistics systems. Permanent aid bases represent preparedness-oriented capacity, whereas temporary aid bases provide flexible response capacity after a disaster. Public and celebrity donations are also modeled as explicit aid flows that can be directed to permanent bases, temporary bases, or affected areas. Accordingly, this study extends the existing literature by jointly considering cost efficiency, unmet demand reduction, shelf-life-dependent perishability, permanent–temporary facility coordination, public aid inflows, and simultaneous demand–supply uncertainty within a unified crisis logistics network design framework.

Table 1. Research literature reviews

Reference	Main decision scope	Uncertainty treatment	Perishability treatment	Explicit perishability	Facility / aid-flow structure	Temporary/public aid structure	Key contribution	Remaining gap relative to this study
Vahdani et al. [16]	Facility location, allocation, and relief distribution	Uncertain disaster conditions	Not explicitly modeled	–	Relief facilities and affected areas	–	Integrated facility-location and allocation decisions in humanitarian logistics	Does not jointly address perishability, public aid flows, and permanent–temporary aid bases
Safaei et al. [11]	Relief facility planning and demand satisfaction	Limited/implicit uncertainty treatment	Not explicitly modeled	–	Relief logistics facilities	–	Balanced cost minimization and demand satisfaction	Limited treatment of perishability and joint demand–supply uncertainty
Nayeem and Lee [8]	Aid distribution and facility allocation	Robust treatment of demand/capacity uncertainty	Not considered	–	Conventional relief distribution network	–	Improved aid distribution under demand/capacity uncertainty	Does not consider age-dependent perishable relief items or donation flows
Boostani et al. [3]	Multi-objective relief supply network	Demand and supply uncertainty	Not explicitly modeled	–	General relief supply network	–	Showed the effect of uncertainty on cost, coverage, and sustainability	Relief items are treated as time-insensitive
Modiri et al. [7]	Relief distribution network design	Robust fuzzy uncertainty	Not considered	–	Disaster relief distribution network	–	Integrated economic, social, and environmental objectives under uncertainty	Does not capture age-structured perishability or facility-type coordination

Table 1 (continued)

Reference	Main decision scope	Uncertainty treatment	Perishability treatment	Explicit perishability	Facility / aid-flow structure	Temporary/public aid structure	Key contribution	Remaining gap relative to this study
Seraji et al. [13]	Two-stage humanitarian logistics planning	Uncertainty in relief operations	Not considered	–	Relief allocation structure	–	Included social performance dimensions under uncertainty	Perishable-item aging and aid-flow routing are not modeled
Wang [18]	Casualty transportation and medical equipment distribution	Global robust optimization	Not considered	–	Emergency medical logistics network	–	Improved emergency medical logistics reliability	Focuses on medical logistics rather than perishable relief networks
Abbasi et al. [1]	Disruption-aware relief network design	Facility failure and disruption uncertainty	Not explicit	–	Emergency supply network	–	Modeled facility failure and pandemic disruptions	Perishability, public aid, and permanent–temporary bases are not jointly addressed
Rajabi et al. [10]	Pharmaceutical supply chain network under COVID-19 disruption	Scenario-based disruption uncertainty	Pharmaceutical products considered, but not age-structured relief perishability	–	Temporary distribution points and backup inventory	✓	Addressed cost–shortage trade-offs in disrupted healthcare supply chains	Limited relevance to disaster relief networks with public aid flows
Zhang et al. [19]	Humanitarian transportation network design	Two-stage Wasserstein DRO	Not considered	–	Road-link strengthening, inventory pre-positioning, and transportation	–	Integrated link strengthening and inventory pre-positioning under ambiguity	Does not consider perishability or public aid inflows

Table 1 (continued)

Reference	Main decision scope	Uncertainty treatment	Perishability treatment	Explicit perishability	Facility / aid-flow structure	Temporary/public aid structure	Key contribution	Remaining gap relative to this study
Wang et al. [17]	Multi-period emergency resource allocation and vehicle routing	Distributionally robust chance constraints	Not considered	–	Allocation-routing structure	–	Modeled multi-period allocation-routing under demand ambiguity	Does not link perishable-item aging with facility-location decisions
Sarmadi and Amiri-Aref [12]	Urban search-and-rescue location-routing	Joint chance-constrained DRO	Not relevant to relief commodities	–	Rescue facility location and team routing	–	Optimized rescue facility location and team routing	Focuses on search-and-rescue, not perishable relief logistics
Zhang et al. [20]	Humanitarian relief logistics network design	Two-stage Wasserstein DRO	Not considered	–	Facility location, inventory pre-positioning, and evacuation planning	–	Integrated facility location, inventory pre-positioning, and evacuation planning	Does not address shelf-life constraints or public/celebrity donations
This study	Crisis logistics network design for perishable relief items	Two-stage robust–probabilistic demand and supply uncertainty	Shelf-life-dependent and age-structured perishability explicitly modeled	✓	Permanent aid bases, temporary aid bases, affected areas, and public/celebrity aid flows	✓	Jointly optimizes facility location, allocation, inventory, shipment, and public aid flows	Addresses the integrated gap in perishability, facility flexibility, public aid, and demand–supply uncertainty

The comparative evidence in Table 1 indicates that prior studies differ not only in their decision scope but also in the way they represent uncertainty and operational realism. Some studies rely on stochastic or scenario-based formulations, which are useful for representing alternative disaster conditions but may provide limited protection against unfavorable deviations within each scenario. In contrast, robust and distributionally robust models improve protection against uncertainty, but they may lead to conservative solutions or require additional ambiguity-set assumptions. This distinction is important for crisis logistics, where both the likelihood of disaster scenarios and the severity of deviations in demand and supply must be reflected in the planning model.

In this regard, the proposed robust–probabilistic approach is positioned as a problem-specific compromise between purely probabilistic and purely robust formulations. The scenario probabilities are used to capture the relative likelihood of disaster scenarios in the objective functions, whereas the robustness-control parameters regulate adverse within-scenario deviations in demand, permanent-base supply, and public aid availability, respectively. Therefore, the probabilistic and robust components play different but complementary roles: the former evaluates expected system performance across scenarios, while the latter protects the network against higher demand and lower available supply within each scenario.

Table 1 also shows that the reviewed studies generally emphasize one or two major modeling dimensions, such as facility location, routing, robust planning, or perishability. However, the simultaneous representation of time-sensitive relief items, flexible aid-base structures, and donation-based supply flows remains limited. The final row of the table clarifies how the present study extends the existing literature by combining these operational features within a unified decision framework rather than treating them as independent modeling components.

2.4.1 Theoretical novelty

The theoretical novelty of this study lies in developing an integrated crisis logistics network design model that jointly captures perishability, permanent–temporary aid-base coordination, public aid flows, and demand–supply uncertainty. The study does not claim to introduce a new optimization paradigm; rather, its contribution is the problem-specific integration of these interdependent features within a single mathematical formulation. The main theoretical novelties are as follows:

Embedding shelf-life-dependent perishability into network design decisions: The model links the limited lifetime of relief items with inventory, shipment, allocation, and unmet-demand decisions, rather than treating perishability as a separate operational constraint.

Developing an age-structured inventory–shipment mechanism for perishable relief items: Relief items are tracked according to their entry period, and shipments are restricted to usable, non-expired inventory batches.

Coordinating permanent and temporary aid bases within one location–allocation framework: The model jointly determines preparedness-oriented permanent bases and response-oriented temporary bases, allowing stable and flexible relief capacities to be designed simultaneously.

Modeling public and celebrity donations as endogenous relief-network flows: Public aid is explicitly formulated as a controllable supply flow that can be routed to permanent bases, temporary bases, or affected areas.

Integrating demand and supply uncertainty in perishable relief logistics: The robust–probabilistic structure considers uncertain relief demand and uncertain supply availability together, enabling shortage risk to be evaluated under scenario-dependent disaster conditions.

2.4.2 Practical novelty

The practical novelty of this study lies in translating the proposed model into a decision-support framework for urban disaster relief planning with perishable items. The model supports emergency managers in designing a relief network that combines preparedness capacity, response flexibility, public aid management, and uncertainty-aware allocation.

Supporting joint planning of permanent and temporary relief infrastructure: The framework helps decision-makers identify where permanent aid bases should be established before a crisis and where temporary relief bases should be deployed during response operations.

Improving the operational management of perishable relief supplies: By considering shelf-life restrictions, the model supports allocation decisions that reduce the risk of delivering unusable or expired relief items.

Providing a structured mechanism for managing public and celebrity donations: The framework helps route donated resources to permanent bases, temporary bases, or affected areas according to network needs and capacity limitations.

Demonstrating applicability in a real metropolitan disaster context: The Tehran case study shows how the model can be used to support relief-base location and perishable-item allocation decisions across urban districts under uncertain demand and supply conditions.

3 Problem definition and modeling

This study considers the design of a crisis logistics network for locating aid bases and distributing perishable relief items to disaster-affected areas under uncertain demand and supply conditions. The primary objective is to ensure timely and effective satisfaction of demand for perishable items by coordinating permanent aid bases, temporary relief bases, and public aid flows, while accounting for shelf-life constraints and limited resources.

The crisis logistics network consists of four main components: permanent aid bases, temporary relief bases, affected areas, and public aid collection sources. In this study, public aid flows refer to the transportation of donated relief items from public and celebrity donor nodes to permanent aid bases, temporary relief bases, or affected areas. Permanent aid bases act as central hubs for receiving, storing, and dispatching relief items, including supplies collected through public and celebrity donations. Temporary relief bases are established in response to a disaster to enhance operational flexibility and reduce delivery times, particularly for perishable items whose usability rapidly deteriorates with delay. Affected areas represent demand points that must be served within strict time windows to ensure the effectiveness of delivered aid.

Public aid flows may be routed to permanent aid bases, temporary relief bases, or directly to affected areas, depending on network requirements and available donated supply. In parallel, perishable relief items are delivered to affected areas through temporary relief bases to improve responsiveness and mitigate spoilage. Transfers of perishable items from permanent aid bases are explicitly constrained by shelf-life considerations, ensuring that all delivered items remain usable upon arrival. By embedding perishability constraints directly into the network structure, the proposed model captures a critical operational characteristic that is often simplified or ignored in conventional humanitarian logistics formulations.

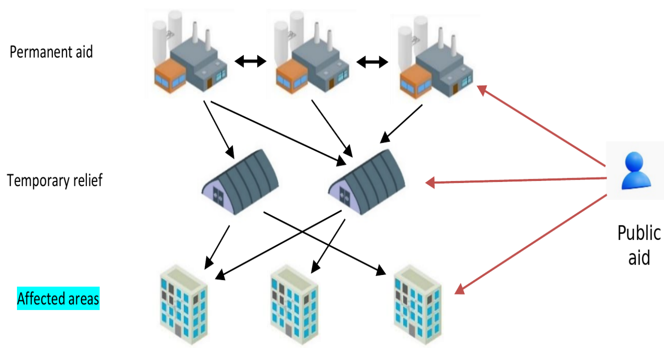

Fig. 1. Proposed crisis logistics network

To address uncertainty in disaster severity, demand levels, and supply availability, a two-stage robust–probabilistic optimization framework is employed. In the first stage, strategic decisions are made regarding the locations of permanent and temporary aid bases, taking into account factors such as accessibility, storage capacity, and spatial proximity. In the second stage, tactical decisions determine the allocation, transportation, and inventory levels of perishable relief items under different disaster scenarios, conditional on realized demand and supply. This structure enables the network to balance preparedness and adaptability while maintaining feasibility across a wide range of uncertain outcomes.

Multiple scenarios with associated occurrence probabilities are considered to represent uncertainty in both demand and supply of relief items. A robust–probabilistic mechanism is used to stabilize the solution space and control deviations between supply and demand across scenarios. The model simultaneously addresses strategic decisions—such as selecting the locations of permanent and temporary aid bases—and tactical decisions—such as determining shipment quantities and inventory levels—while optimizing two conflicting objectives: minimizing the total cost of the crisis logistics network and minimizing the maximum unmet demand in affected areas.

For clarity, the overall structure of the proposed crisis logistics network and the interactions among its main components are illustrated in Fig. 1.

The formulation of the crisis logistics network design problem is based on the following assumptions:

1. Aid contributed by the public can be dispatched to permanent aid bases, temporary relief bases, or directly to affected areas, depending on the crisis conditions.
2. Relief items are perishable, and each product is associated with a predefined shelf life.
3. The criteria for establishing permanent and temporary relief bases are predetermined.
4. Demand and supply of relief items are scenario-dependent and uncertain.
5. Transportation of relief items between permanent aid bases is permitted.
6. Transportation costs are assumed to be homogeneous across product types and are calculated on a per-kilometer basis, reflecting an average cost per standardized shipment unit.

In this study, transportation costs are modeled as uniform across product types and are expressed as an average cost per kilometer per standardized shipment unit (e.g., per pallet or vehicle load). This simplification is motivated by two considerations. First, in many humanitarian operations, heterogeneous relief items are consolidated into mixed loads, and transportation is charged at the vehicle or route level rather than at the item level. Second, reliable item-specific transportation cost data for different relief products were not available for the case study, while the primary focus of this study is on network design under uncertainty and perishability constraints. Therefore, adopting a uniform per-kilometer transportation cost allows us to capture the dominant cost component (distance) without introducing additional parameters that are difficult to estimate in practice.

To facilitate the modeling process, the relevant notations are defined as follows:

Indices and sets:

I	Set of permanent aid bases
J	Set of temporary aid bases
K	Set of affected (demand) areas
L	Set of public and celebrity aid collection nodes, indexed by l
P	Set of relief item types
t	Index of time period (crisis period), $t \in \{1,2,\ldots,\|T\|\}$
r	Index of the period in which an inventory batch enters a temporary relief base. For a batch used in shipment period t, its age is $t-r+1$, and only batches satisfying $\max\{1, t-v_p+1\} \leq r \leq t$ are usable.
S	Set of disaster scenarios
a, b	Generic indices of network nodes belonging to $I \cup J \cup K \cup L$

Parameters:

φ_i	Fixed cost of establishing a permanent base i
ϑ_j	Fixed cost of establishing a temporary base j
h_{jp}	Holding cost of relief item p at temporary base j
$\zeta_{a,b}$	Distance from network node a to network node b, where $a,b \in I \cup J \cup K \cup L$
ψ	Transportation cost per kilometer per standardized unit of relief item
$\bar{d}_{kpts}$	Nominal demand for relief item p in affected area k during period t under scenario s.
v_p	Shelf life of relief item p, measured in discrete time periods.
$\bar{\rho}_{ipts}$	Nominal available supply of relief item p at permanent aid base i in period t under scenario s.
$\bar{\gamma}_{lpts}$	Nominal available quantity of donated relief item p at donor node l in period t under scenario s.
$\bar{\gamma}_{lpts}$	Uncertain available quantity of donated relief item p at donor node l in period t under scenario s; it refers exclusively to donated relief availability and is distinct from the operational capacity of temporary relief bases.
$\bar{\rho}_{ipts}$	Uncertain available supply of relief item p at permanent aid base i in period t under scenario s.
$\tilde{d}_{kpts}$	Uncertain demand for relief item p in affected area k during period t under scenario s.

c_{jt}	Capacity to provide relief items by the temporary base j at the moment of crisis t
b_{jpt}	Maximum storage capacity of relief items p in the temporary base j at the moment of crisis t
δ_{jpt}	Safety stock level of relief items p in temporary base j at the moment of crisis t
p_s	Probability of occurrence of disaster scenario s, where s$\in\mathscr{S}$, $\sum_{s\in S} p_s = 1$.
M^{out}_{ipts}	Data-dependent upper bound on the total outbound flow of relief item p from permanent aid base i in period t under scenario s.
M^{in}_{ipts}	Data-dependent upper bound on the total inbound flow of relief item p to permanent aid base i in period t under scenario s.

Decision variables:

X_{ijpts}	Quantity of relief item p transferred from permanent base i to temporary base j in period t under scenario s.
Y_{jkpts}	Quantity of relief item p transferred from temporary base j to affected area k in period t under scenario s.
Z_{ikpts}	Quantity of relief item p transferred from permanent base i to affected area k in period t under scenario s.
$W_{ii'pts}$	Quantity of relief item p transferred from permanent base i to permanent base i' in period t under scenario s.
U_{jkptrs}	Quantity of relief item p shipped from temporary relief base j to affected area k in period t, drawn from the inventory batch that entered the temporary base in period r, under scenario s.
A_{lipts}	Quantity of donated relief item p transported from donor node l to permanent aid base i in period t under scenario s.
V_{ljpts}	Quantity of donated relief item p transported from donor node l to temporary aid base j in period t under scenario s.
O_{lkpts}	Quantity of donated relief item p transported from donor node l directly to affected area k in period t under scenario s.
$IN_{j,p,t,r,s}$	Inventory of item p at temporary base j in period t, from the batch that entered in period r (age $t-r+1$), under scenario s.
G_i	Binary variable equal to 1 if permanent base i is established, and 0 otherwise.
E_j	Binary variable equal to 1 if temporary base j is established, and 0 otherwise.

The bi-objective mathematical model for the crisis logistics network, aimed at locating aid bases, is presented as follows:

$$
\begin{aligned}
\min \quad & \sum_{i\in I} \varphi_i G_i + \sum_{j\in J} \vartheta_j E_j \\
& + \sum_{s\in S} p_s \Bigg[\sum_{i\in I}\sum_{j\in J}\sum_{p\in P}\sum_{t\in T} \psi \zeta_{ij} X_{ijpts} + \sum_{j\in J}\sum_{k\in K}\sum_{p\in P}\sum_{t\in T} \psi \zeta_{jk} Y_{jkpts} \\
& \quad + \sum_{i\in I}\sum_{k\in K}\sum_{p\in P}\sum_{t\in T} \psi \zeta_{ik} Z_{ikpts} + \sum_{i\in I}\sum_{i'\in I}\sum_{p\in P}\sum_{t\in T} \psi \zeta_{ii'} W_{ii'pts} \\
& \quad + \sum_{l\in L}\sum_{i\in I}\sum_{p\in P}\sum_{t\in T} \psi \zeta_{li} A_{lipts} + \sum_{l\in L}\sum_{j\in J}\sum_{p\in P}\sum_{t\in T} \psi \zeta_{lj} V_{ljpts} \\
& \quad + \sum_{l\in L}\sum_{k\in K}\sum_{p\in P}\sum_{t\in T} \psi \zeta_{lk} O_{lkpts} + \sum_{j\in J}\sum_{p\in P}\sum_{t\in T}\sum_{r\in T} h_{jp} IN_{j,p,t,r,s} \Bigg]
\end{aligned} \tag{1}
$$

$$
\min \max_{\substack{k\in K,\, p\in P,\\ t\in T,\, s\in S}} \left\{ \bar{d}_{kpts} - \left(\sum_{j\in J} Y_{jkpts} + \sum_{i\in I} Z_{ikpts} + \sum_{l\in L} O_{lkpts} \right) \right\} \tag{2}
$$

s.t.

$$
\bar{d}_{kpts} - \left(\sum_{j\in J} Y_{jkpts} + \sum_{i\in I} Z_{ikpts} + \sum_{l\in L} O_{lkpts} \right) \geq 0, \quad \forall k\in K,\ p\in P,\ t\in T,\ s\in S \tag{3}
$$

$$
IN_{j,p,1,1,s} = \sum_{i\in I} X_{ijp1s} + \sum_{l\in L} V_{ljp1s} - \sum_{k\in K} Y_{jkp1s}, \quad \forall j\in J,\ p\in P,\ s\in S \tag{4}
$$

$$
\sum_{r=1}^{t} IN_{j,p,t,r,s} = \sum_{r=1}^{t-1} IN_{j,p,t-1,r,s} + \sum_{i\in I} X_{ijpts} + \sum_{l\in L} V_{ljpts} - \sum_{k\in K} Y_{jkpts}, \quad \forall j\in J,\ p\in P,\ 2\leq t < v_p,\ s\in S \tag{5}
$$

$$
\sum_{r=t-v_p+1}^{t} IN_{j,p,t,r,s} = \sum_{r=t-v_p+1}^{t-1} IN_{j,p,t-1,r,s} + \sum_{i\in I} X_{ijpts} + \sum_{l\in L} V_{ljpts} - \sum_{k\in K} Y_{jkpts}, \quad \forall j\in J,\ p\in P,\ t\geq v_p,\ s\in S \tag{6}
$$

$$
Y_{jkpts} = \sum_{r=1}^{t} U_{jkptrs}, \quad \forall j\in J,\ k\in K,\ p\in P,\ t < v_p,\ s\in S \tag{7}
$$

$$
Y_{jkpts} = \sum_{r=t-v_p+1}^{t} U_{jkptrs}, \quad \forall j\in J,\ k\in K,\ p\in P,\ t\geq v_p,\ s\in S \tag{8}
$$

$$
IN_{j,p,t,t,s} = \sum_{i\in I} X_{ijpts} + \sum_{l\in L} V_{ljpts} - \sum_{k\in K} U_{jkptts}, \quad \forall j\in J,\ p\in P,\ t\in T,\ s\in S \tag{9}
$$

$$
IN_{j,p,t,r,s} = IN_{j,p,t-1,r,s} + \sum_{l\in L} V_{ljpts} - \sum_{k\in K} U_{jkptrs}, \quad \forall j\in J,\ p\in P,\ r < t,\ t-r < v_p,\ s\in S \tag{10}
$$

$$
\sum_{l\in L} A_{lipts} + \sum_{i'\in I} W_{i'ipts} = \sum_{i'\in I} W_{ii'pts} + \sum_{k\in K} Z_{ikpts}, \quad \forall i\in I,\ p\in P,\ t\in T,\ s\in S \tag{11}
$$

$$
\sum_{j\in J} X_{ijpts} \leq \bar{\rho}_{ipts} G_i, \quad \forall i\in I,\ p\in P,\ t\in T,\ s\in S \tag{12}
$$

$$
\sum_{k\in K}\sum_{p\in P} Y_{jkpts} \leq c_{jt} E_j, \quad \forall j\in J,\ t\in T,\ s\in S \tag{13}
$$

$$\sum_{r=1}^{t} IN_{j,p,t,r,s} \le b_{jpt} E_j, \quad \forall j \in J, p \in P, t \in T, s \in S \tag{14}$$

$$\sum_{r=1}^{t} IN_{j,p,t,r,s} \ge \delta_{jpt} E_j, \quad \forall j \in J, p \in P, t \in T, s \in S \tag{15}$$

$$\sum_{j \in J} V_{ljpts} + \sum_{k \in K} O_{lkpts} + \sum_{i \in I} A_{lipts} \le \bar{\gamma}_{lpts}, \quad \forall l \in L, p \in P, t \in T, s \in S \tag{16}$$

$$\sum_{i' \in I} W_{ii'pts} + \sum_{k \in K} Z_{ikpts} \le M^{out}_{ipts} G_i, \quad \forall i \in I, p \in P, t \in T, s \in S \tag{17}$$

$$\sum_{l \in L} A_{lipts} + \sum_{i' \in I} W_{i'ipts} \le M^{in}_{ipts} G_i, \quad \forall i \in I, p \in P, t \in T, s \in S \tag{18}$$

$$IN_{j,p,t,r,s} = 0, \quad \forall j \in J, p \in P, t < r, s \in S \tag{19}$$

$$X_{ijpts}, Y_{jkpts}, Z_{ikpts}, W_{ii'pts}, U_{jkptrs}, A_{lipts}, V_{ljpts}, O_{lkpts}, IN_{j,p,t,r,s} \ge 0, \tag{20}$$

for all applicable $i, i' \in I$, $j \in J$, $k \in K$, $p \in P$, $r, t \in T$, $s \in S$, and $l \in L$

$$G_i, E_j \in \{0,1\}, \quad \forall i \in I, j \in J \tag{21}$$

Equation (1) defines the total cost of the crisis logistics network, encompassing facility location costs, transportation costs, and inventory holding costs associated with perishable relief items. Equation (2) specifies the second objective function, which aims to minimize the maximum unmet demand over all affected areas, items, periods, and scenarios. Constraint (3) guarantees that the unmet demand term is nonnegative in each (k, p, t, s) combination and prevents oversupplying any demand point. Consequently, the quantity inside the max operator can be interpreted consistently as the shortage (unmet demand), and the second objective can be clearly understood as minimizing its maximum value.

Constraints (4)–(6) model the inventory dynamics of perishable items at temporary relief bases while explicitly accounting for shelf-life limitations. Constraint (4) gives the initial-period inventory balance. Because $t = 1$, only the batch entering in period $r = 1$ can exist, and the corresponding inventory is $IN_{j,p,1,1,s}$. Constraint (5) applies to the early periods $2 \le t < v_p$, during which all previously received batches remain usable, whereas Constraint (6) applies for $t \ge v_p$, when only batches received from period $t - v_p + 1$ onward remain usable. Constraints (7) and (8) link the aggregate shipment variable Y_{jkpts} to the batch-specific shipment variable U_{jkptrs}. The index r denotes the period in which a batch enters temporary relief base j, whereas t denotes the shipment period. Hence, the age of a batch received in period r and used in period t is $t - r + 1$, and the admissible entry periods satisfy $\max\{1, t - v_p + 1\} \le r \le t$. This structure prevents expired or not-yet-received batches from being shipped. Constraints (9) and (10) further enforce inventory balance and batch availability at temporary bases.

Constraint (11) represents flow balance at each permanent aid base. The variable A_{lipts} denotes the donated quantity of item p received by permanent aid base i from donor node l in period t under scenario s. Together with inbound inter-base transfers, these supplies are dispatched either to other permanent bases or directly to affected areas. Constraint (12) limits shipments from an opened permanent base by its nominal available supply. Constraint (13) limits the aggregate handling capacity of each temporary relief base across all affected areas and relief items. Constraints (14) and (15) impose, respectively, maximum storage capacity and minimum safety-stock requirements. Constraint (16) limits the total allocation of donated relief items from each public or celebrity aid collection node. For each donor node l, item p, period t, and scenario s, the sum of donated flows to permanent bases, temporary bases, and affected areas cannot exceed the nominal aid availability $\bar{\gamma}_{lpts}$. The routing variables A_{lipts}, V_{ljpts}, and O_{lkpts} remain destination-specific, and their corresponding origin–destination distances are included in the transportation cost.

Constraints (17) and (18) link permanent-base opening decisions to outbound and inbound flows. If $G_i = 0$, permanent base i cannot send or receive relief items. The Big-M coefficients are data-dependent rather than arbitrary. The maximum feasible inbound flow to permanent aid base i is bounded by the total nominal public-aid availability plus the nominal supplies that could be transferred from the other permanent bases:

$$M^{in}_{ipts} = \sum_{l\in L} \bar{\gamma}_{lpts} + \sum_{\substack{i'\in I\\ i'\neq i}} \bar{\rho}_{i'pts}.$$

The corresponding outbound bound is

$$M^{out}_{ipts} = \bar{\rho}_{ipts} + M^{in}_{ipts}.$$

Because supply uncertainty is modeled only through downward deviations from nominal supply, $\bar{\rho}_{ipts}$ and $\bar{\gamma}_{lpts}$ are valid upper bounds for all uncertainty realizations considered here. These coefficients tighten Constraints (17) and (18), reduce numerical instability, and improve branch-and-bound efficiency. Constraint (19) enforces temporal consistency by preventing inventory from existing before its replenishment period. Finally, Constraints (20) and (21) define the domains of the continuous and binary decision variables.

The proposed formulation adopts a bi-objective structure to balance economic efficiency and humanitarian effectiveness. The first objective function (Z_1) seeks to minimize the overall operational and infrastructure costs of the crisis logistics network, while the second objective function (Z_2) focuses on minimizing the maximum level of unmet demand in disaster-affected areas. By jointly considering facility location decisions, capacity and storage constraints, perishability effects, and donation flows, the model provides decision-makers with a structured framework for evaluating trade-offs between cost containment and rapid, reliable relief delivery under uncertain conditions.

3.1 Linearization of the mathematical model

The second objective function in Equation (2) contains a maximum operator over the unmet demand associated with all affected areas, relief items, periods, and scenarios. To obtain an equivalent linear formulation, an auxiliary variable θ is introduced to represent the maximum unmet demand. The epigraph reformulation of Equation (2) is expressed as follows:

$$\min \quad \theta \tag{22}$$

$$\text{s.t.} \quad \theta \geq \bar{d}_{kpts} - \sum_{j\in J} Y_{jkpts} - \sum_{i\in I} Z_{ikpts} - \sum_{l\in L} O_{lkpts}, \quad \forall k\in K, p\in P, t\in T, s\in S, \tag{23}$$

together with Equation (1) and Constraints (3)–(21).

Constraint (23) ensures that θ is greater than or equal to the unmet demand for every affected-area, relief-item, period, and scenario combination. Since Equation (22) minimizes θ, its optimal value becomes equal to the maximum unmet demand appearing in Equation (2). Therefore, Equations (22) and (23) constitute an equivalent linear epigraph reformulation of the original second objective function.

3.2 Two-stage robust-probabilistic method

In the proposed crisis logistics network, demand for relief items and supply availability are uncertain and scenario-dependent. To address this issue, a two-stage robust–probabilistic optimization framework is developed for locating aid bases and allocating perishable relief items while considering public aid flows.

The model integrates scenario-based probabilistic representation with bounded uncertainty control. Scenario probabilities p_s represent the likelihood of disaster conditions, while robustness-control parameters α, β, and δ regulate the level of protection against adverse deviations in demand and supply. This results in a hybrid robust–probabilistic formulation.

First-stage decisions: G_i is the location decision for permanent aid base i, and E_j is the location decision for temporary aid base j.

These decisions are made before uncertainty realization and define the network structure.

Second-stage decisions: $X_{ijpts}, Y_{jkpts}, Z_{ikpts}, W_{ii'pts}$ are scenario-dependent relief-flow allocation decisions; $A_{lipts}, V_{ljpts}, O_{lkpts}$ are scenario-dependent public-aid allocation decisions; and $U_{jkptrs}, IN_{j,p,t,r,s}$ are scenario-dependent shipment and inventory decisions.

These decisions are made after the realization of uncertainty and are indexed by $s \in S$.

Uncertainty parameters:

Demand and supply uncertainty are defined as:

$$\begin{aligned}
\tilde{d}_{kpts} &\in \left[\bar{d}_{kpts}, (1+\alpha)\bar{d}_{kpts}\right], \\
\tilde{\rho}_{ipts} &\in \left[(1-\beta)\bar{\rho}_{ipts}, \bar{\rho}_{ipts}\right], \\
\tilde{\gamma}_{lpts} &\in \left[(1-\delta)\bar{\gamma}_{lpts}, \bar{\gamma}_{lpts}\right].
\end{aligned} \tag{24}$$

where α, β, and δ are robustness-control parameters. Here, $\bar{d}_{kpts}$, $\bar{\rho}_{ipts}$, and $\bar{\gamma}_{lpts}$ denote the nominal relief demand, the nominal available supply at permanent aid base i, and the nominal availability of donated relief items at public and celebrity aid collection node l, respectively. These nominal values serve as the reference parameters for constructing the bounded uncertainty sets, while α, β, and δ determine the maximum allowable adverse deviations.

The uncertainty sets are intentionally asymmetric to reflect the nature of humanitarian logistics disruptions. Demand uncertainty is modeled through upward deviations from its nominal value, whereas supply uncertainty is represented by downward deviations from the nominal available supply, corresponding to the worst-case conditions considered in the proposed robust–probabilistic framework.

Objective functions:

$$\begin{aligned}
\min\ \omega_1 = {} & \sum_{i\in I}\varphi_i G_i + \sum_{j\in J}\vartheta_j E_j \\
& + \sum_{s\in S} p_s \Bigg[\sum_{i\in I}\sum_{j\in J}\sum_{p\in P}\sum_{t\in T}\psi\zeta_{ij}X_{ijpts} + \sum_{j\in J}\sum_{k\in K}\sum_{p\in P}\sum_{t\in T}\psi\zeta_{jk}Y_{jkpts} \\
& \quad + \sum_{i\in I}\sum_{k\in K}\sum_{p\in P}\sum_{t\in T}\psi\zeta_{ik}Z_{ikpts} + \sum_{i\in I}\sum_{i'\in I}\sum_{p\in P}\sum_{t\in T}\psi\zeta_{ii'}W_{ii'pts} \\
& \quad + \sum_{l\in L}\sum_{i\in I}\sum_{p\in P}\sum_{t\in T}\psi\zeta_{li}A_{lipts} + \sum_{l\in L}\sum_{j\in J}\sum_{p\in P}\sum_{t\in T}\psi\zeta_{lj}V_{ljpts} \\
& \quad + \sum_{l\in L}\sum_{k\in K}\sum_{p\in P}\sum_{t\in T}\psi\zeta_{lk}O_{lkpts} + \sum_{j\in J}\sum_{p\in P}\sum_{t\in T}\sum_{r\in T}h_{jp}IN_{j,p,t,r,s} \Bigg]
\end{aligned} \tag{25}$$

$$\min\ \omega_2 = \theta \tag{26}$$

s.t.

$$\theta \geq (1+\alpha)\bar{d}_{kpts} - \left(\sum_{j\in J} Y_{jkpts} + \sum_{i\in I} Z_{ikpts} + \sum_{l\in L} O_{lkpts} \right), \quad \forall k \in K,\, p \in P,\, t \in T,\, s \in S \tag{27}$$

$$\sum_{j\in J} X_{ijpts} \leq (1-\beta)\bar{\rho}_{ipts} G_i, \quad \forall i \in I,\, p \in P,\, t \in T,\, s \in S \tag{28}$$

$$\sum_{j\in J} V_{ljpts} + \sum_{k\in K} O_{lkpts} + \sum_{i\in I} A_{lipts} \leq (1-\delta)\bar{\gamma}_{lpts}, \quad \forall l \in L,\, p \in P,\, t \in T,\, s \in S \tag{29}$$

Constraints (3)–(10), (12)–(14), and (16)–(18) also apply.

In Equations (25)–(29), uncertainty is incorporated through a hybrid robust–probabilistic framework. The scenario probabilities p_s represent the likelihood of different disaster scenarios and are used to evaluate the expected system performance across all scenarios. In contrast, the parameters α, β, and δ are robustness-control coefficients that define the size of the uncertainty sets and regulate the level of conservatism of the model.

Specifically, α controls the upward deviation of relief demand, whereas β and δ control the downward deviations of the available supply at permanent aid bases and the availability of donated relief items at public and celebrity aid collection nodes, respectively. Accordingly, demand and supply are assumed to vary within the bounded uncertainty sets $\tilde{d}_{kpts} \in [\bar{d}_{kpts}, (1+\alpha)\bar{d}_{kpts}]$, $\tilde{\rho}_{ipts} \in [(1-\beta)\bar{\rho}_{ipts}, \bar{\rho}_{ipts}]$, and $\tilde{\gamma}_{lpts} \in [(1-\delta)\bar{\gamma}_{lpts}, \bar{\gamma}_{lpts}]$. Therefore, the model simultaneously accounts for the probabilistic occurrence of disaster scenarios and protection against adverse demand and supply deviations. When $\alpha = \beta = \delta = 0$, the uncertainty sets collapse to their nominal values and the proposed model reduces to the nominal scenario-based formulation. Increasing these parameters enlarges the uncertainty sets, resulting in more conservative solutions that improve protection against higher demand and lower supply availability, albeit at the expense of higher logistics costs.

3.3 Calibration of uncertainty-control parameters

The uncertainty-control parameters α, β, and δ are used to regulate the conservatism of the proposed robust–probabilistic model. These parameters are not additional random variables and should not be interpreted as statistical confidence levels. Rather, they are robustness-control coefficients that adjust scenario-based demand and supply values toward adverse realizations. Parameter α controls the upward deviation of relief demand, β controls the downward deviation of supply from permanent aid bases, and δ controls the downward deviation of public aid availability. When these parameters increase, the model represents more severe disaster conditions through higher demand and lower available supply.

In practical applications, these parameters can be calibrated using historical disaster records, expert judgment, or planning-level stress assumptions. If sufficient empirical data are available, α can be estimated from the relative deviation between an upper demand quantile and the expected demand, while β and δ can be estimated from the relative deviation between expected supply and a conservative lower-bound supply estimate. The uncertainty-control parameters are calculated according to Equations (30)–(32):

$$\alpha = \frac{D^U - D^E}{D^E}, \tag{30}$$

Table 2. Calibration logic of uncertainty-control parameters

Parameter	Role in the model	Adverse adjustment	Possible calibration rule	Interpretation
α	Demand uncertainty-control parameter	Increases effective demand	$(D^U - D^E)/D^E$	Percentage increase from expected demand to conservative upper demand
β	Supply uncertainty-control parameter	Reduces supply from permanent aid bases	$(S^E - S^L)/S^E$	Percentage reduction from expected supply to conservative lower supply
δ	Public aid uncertainty-control parameter	Reduces public aid availability	$(Q^E - Q^L)/Q^E$	Percentage reduction from expected public aid to conservative lower public aid

$$\beta = \frac{S^E - S^L}{S^E}, \tag{31}$$

$$\delta = \frac{Q^E - Q^L}{Q^E}. \tag{32}$$

where D^E denotes the expected demand, D^U represents a conservative upper demand estimate, S^E denotes the expected supply from permanent aid bases, S^L represents a conservative lower supply estimate, Q^E denotes the expected public aid availability, and Q^L represents a conservative lower public aid estimate.

The calibration logic of the uncertainty-control parameters is summarized in Table 2. This calibration structure clarifies that α, β, and δ are not arbitrarily selected but represent controllable levels of demand increase and supply reduction. In the present case study, these parameters are treated as robustness-control parameters, and their effects are further evaluated through sensitivity analysis.

4 Solution method

To solve the proposed bi-objective mathematical model, the ε-constraint method is employed, specifically its enhanced version to improve solution diversity and overcome the weaknesses of the standard ε-constraint approach. This method is widely used for generating Pareto-optimal solutions in multi-objective optimization problems. In the enhanced ε-constraint approach, one objective function is optimized while the others are converted into constraints with an upper bound ε. The lexicographic optimization technique is incorporated to ensure a uniform spread of Pareto solutions.

In the previous section, the modeling of a crisis logistics network was discussed for the location of aid bases, considering perishable items and public aid flows under uncertainty. Since the problem involves two conflicting objective functions, the enhanced ε-constraint method is employed to construct the Pareto front and generate a range of efficient solutions. The ε-constraint method is enhanced by incorporating the lexicographic approach for each objective function, which allows the calculation of values in the final result table. In this approach, the sub-objective function constraints are converted into equalities through the use of auxiliary variables. In optimization with the lexicographic method, the payoff table is first generated by optimizing each objective individually. After optimizing one objective function, the subsequent objective function is optimized while preserving the optimal value of the previously optimized objective, thereby obtaining lexicographically efficient extreme points. These extreme values determine the range r_2 used to construct the ε-grid. For the bi-objective minimization problem, the first objective f_1 is retained as the primary objective, whereas the second objective is converted into an ε-constraint. To avoid weakly efficient solutions, a non-negative slack variable s_2 is introduced and incorporated into the objective function through a small augmentation coefficient τ¿0. The resulting enhanced ε-constraint formulation for each grid point is:

$$\begin{aligned} \min \quad & \omega_1 - \tau \frac{s_2}{r_2} \\ \text{s.t.} \quad & \omega_2 + s_2 = \varepsilon_2^m, \\ & x \in \Omega, \quad s_2 \geq 0 \end{aligned} \tag{33}$$

where s_2 is the non-negative slack variable associated with the second objective, τ is a sufficiently small positive augmentation coefficient, r_2 is the range of the second objective obtained from the payoff table, and ε_2^m is the bound imposed on the second objective at iteration m. The set Ω represents the complete feasible region of the robust–probabilistic model.

5 Case study

To demonstrate the practical applicability and effectiveness of the proposed model, a real-world case study is conducted. The study focuses on Tehran, a large metropolitan area comprising 22 municipal districts and covering approximately 730 square kilometers. Over the past five decades, the city's population has increased from about three million to more than nine million inhabitants, reflecting rapid urban expansion and mounting pressure on critical infrastructure and emergency management systems.

Existing studies and official assessments consistently identify Tehran as highly vulnerable to large-scale natural disasters, particularly earthquakes, which are expected to cause extensive human casualties and substantial economic losses. In such a context, the strategic placement and operational coordination of permanent and temporary aid bases play a pivotal role in strengthening emergency response capacity and mitigating post-disaster impacts. Accordingly, this case study examines the performance of a crisis logistics network designed to support the timely and efficient distribution of relief items in a densely populated urban environment.

In the numerical implementation, each municipal district is considered a potential candidate location for both permanent and temporary aid bases. At the same time, all districts are treated as demand nodes representing affected areas. The severity of damage in each district is assumed to be directly proportional to its population size, capturing the heightened exposure and vulnerability of densely populated regions during major disaster events. This assumption enables the model to prioritize relief allocation to areas with the highest potential humanitarian impact.

The spatial structure of the study area is illustrated in Fig. 2, which depicts the geographical distribution of the 22 municipal districts. Pairwise distances between districts, used to compute transportation costs, are reported in Table 4. In addition, key model parameters are specified under three disaster scenarios—low-, medium-, and high-intensity events—to represent varying levels of incident severity and operational stress. The corresponding scenario-dependent parameter values are summarized in Table 3.

To enhance the robustness and credibility of the analysis, the proposed model is evaluated across all three scenarios. This scenario-based assessment enables a systematic examination of network per-

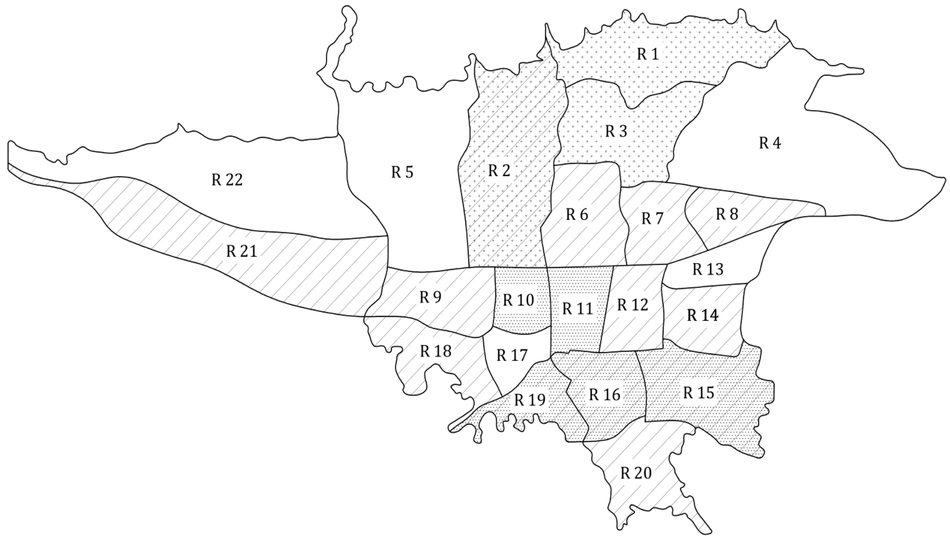

Fig. 2. Visual representation of Tehran metropolis

formance under a broad spectrum of operating conditions, ranging from moderate disruptions to severe crisis situations. By explicitly linking damage severity to population concentration, the model ensures that relief resources are allocated in accordance with humanitarian priorities. Overall, this data-driven and scenario-oriented case study provides actionable insights for urban emergency planners and policymakers and demonstrates the potential of the proposed framework to support disaster preparedness and response planning in large metropolitan regions. Notably, in the case study, public and celebrity donations are represented by a single aggregated aid-collection node, i.e., L=$\{1\}$. Therefore, only the donation origin is aggregated, whereas destination-specific allocations to permanent bases, temporary bases, and affected areas remain explicitly modeled.

Table 3 summarizes the parameter ranges used in the Tehran case study. In Table 3, U(a, b) denotes a uniform distribution over the interval [a,b], where a and b represent the lower and upper bounds of the corresponding parameter, respectively. For example, U(150,250) indicates that the parameter takes values uniformly within the interval from 150 to 250.

Also, the distance of 22 districts of Tehran metropolis from each other is presented in Table 4.

Table 3 indicates that as the severity of the disaster increases, both the extent of damage and the demand for perishable relief items rise accordingly. Simultaneously, higher levels of destruction tend to constrain the effective delivery of aid, particularly supplies originating from permanent aid bases and public aid flow sources, due to infrastructure disruption and reduced accessibility. Table 5 reports the set of efficient solutions obtained for a disaster duration of 10 hours and considers two categories of perishable relief items: warm items (cooked meals with an energy content of 243 calories and a shelf life of 2 hours) and dry items (including bread, rice, and canned goods with an energy content of 456 calories and a shelf life of 5 hours).

As reported in Table 5, an increase in the number of temporary aid bases, along with higher inventory holding costs for perishable items, is associated with a reduction in the level of unmet demand in

Table 3. Interval limits of problem parameters in different scenarios

Parameter	Parameter value		
φ_i	$U(200000, 300000)\$$		
ϑ_j	$U(25000, 35000)\$$		
h_{jp}	$U(1,5)\$/\text{unit}$		
ψ	$U(1,3)\$/km$		
v_p	$U(1,6)h$		
c_{jt}	$U(1000, 4000)kg$		
b_{jpt}	$U(200, 500)kg$		
δ_{jpt}	$U(50, 120)kg$		
	Mild disaster	Moderate disaster	Severe disaster
$\tilde{d}_{kpts}$	$U(150, 250)kg$	$U(300, 500)kg$	$U(600, 800)kg$
$\tilde{\rho}_{ipts}$	$U(2000, 3000)kg$	$U(1800, 2000)kg$	$U(1500, 1800)kg$
$\tilde{\gamma}_{lpts}$	$U(300, 500)kg$	$U(200, 300)kg$	$U(150, 200)kg$
p_s	0.3	0.4	0.3

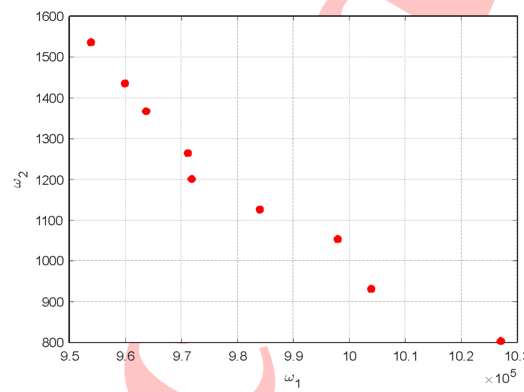

Fig. 3. Pareto front obtained from solving the case study

the affected areas. This result indicates that expanding temporary response capacity enhances network responsiveness and mitigates shortages of time-sensitive relief items. In particular, increasing the number of temporary relief bases from seven in efficient solution (1) to ten in efficient solution (9) leads to an approximately 47.7% reduction in maximum unmet demand.

Fig. 3 illustrates the resulting Pareto front obtained from solving the case study, highlighting the trade-off between total network cost and unmet demand and providing decision-makers with a range of efficient solutions reflecting different priority structures.

To examine and validate the outputs of the model, the first efficient solution is selected as a representative example, and the corresponding locations of permanent and temporary aid bases are illustrated in Fig. 4.

As shown in Fig. 4, the first efficient solution selects districts 2, 7, and 15 as permanent aid-base locations and districts 3, 6, 10, 14, 19, 20, and 21 as temporary aid-base locations. This configuration yields a total crisis-logistics cost of USD 953,811.99 and a maximum unmet demand of 1,536.24 kg. The corresponding demand coverage across Tehran's 22 districts is reported in Table 6.

Table 4. Distance of 22 districts of Tehran metropolis from each other

	1	2	3	4	5	6	7	8	9	10	11	12	13	14	15	16	17	18	19	20	21	22
1	-	15.4	6.9	14.5	19.7	14.1	15.1	14.6	27.4	24.3	20.2	21.2	19.8	23.7	24.1	26.4	24.7	32.2	28.2	31.2	33.7	28.5
2	15.4	-	12.7	19.6	4.5	10.6	14.3	18.1	12.7	9.3	13.0	18.2	22.1	26.0	27.3	21.5	13.4	17.4	16.6	27.1	18.3	17.3
3	6.9	12.7	-	13.6	13.9	7.5	7.9	13.5	22.6	19.5	16.3	13.4	19.3	23.2	23.5	18.7	18.6	24.1	22.0	30.6	27.5	23.5
4	14.5	19.6	13.6	-	22.1	17.1	12.5	6.7	28.5	27.1	23.7	18.8	6.9	10.8	17.1	23.2	28.0	34.7	27.9	23.6	35.9	34.2
5	19.7	4.5	13.9	22.1	-	13.5	17.3	21.1	14.8	13.0	16.5	22.9	25.1	27.9	30.1	24.4	20.3	19.6	20.2	30.0	16.8	13.7
6	14.1	10.6	7.5	17.1	13.5	-	5.6	10.4	15.0	9.0	6.9	10.2	12.1	14.2	15.3	12.8	12.6	19.7	16.1	22.3	20.0	25.6
7	15.1	14.3	7.9	12.5	17.3	5.6	-	6.1	22.1	20.6	10.9	8.5	7.8	12.7	13.0	13.7	20.9	31.5	27.7	20.1	27.2	27.4
8	14.6	18.1	13.5	6.7	21.1	10.4	6.1	-	25.5	14.8	15.7	15.4	2.8	7.7	14.1	20.4	24.9	32.9	26.1	21.5	30.6	33.0
9	27.4	12.7	22.6	28.5	14.8	15.0	22.1	25.5	-	9.0	13.1	20.5	33.6	31.0	28.3	21.8	9.9	7.1	12.2	21.9	5.7	25.6
10	24.3	9.3	19.5	27.1	13.0	9.0	20.6	14.8	9.0	-	4.2	9.9	15.1	16.7	17.1	11.3	4.2	10.6	10.7	16.9	14.6	24.5
11	20.2	13.0	16.3	23.7	16.5	6.9	10.9	15.7	13.1	4.2	-	5.3	21.0	13.3	13.6	7.8	5.2	9.2	9.4	15.6	17.7	29.0
12	21.2	18.2	13.4	18.8	22.9	10.2	8.5	15.4	20.5	9.9	5.3	-	15.5	9.1	9.9	7.5	7.9	16.6	11.4	8.5	21.2	40.1
13	19.8	22.1	19.3	6.9	25.1	12.1	7.8	2.8	33.6	15.1	21.0	15.5	-	4.8	12.8	18.9	23.7	30.4	23.6	19.3	46.2	32.5
14	23.7	26.0	23.2	10.8	27.9	14.2	12.7	7.7	31.0	16.7	13.3	9.1	4.8	-	8.3	12.7	17.2	25.9	19.2	14.9	41.8	49.4
15	24.1	27.3	23.5	17.1	30.1	15.3	13.0	14.1	28.3	17.1	13.6	9.9	12.8	8.3	-	7.8	12.3	21.4	14.6	10.3	37.3	44.9
16	26.4	21.5	18.7	23.2	24.4	12.8	13.7	20.4	21.8	11.3	7.8	7.5	18.9	12.7	7.8	-	9.6	16.7	10.0	4.9	32.6	40.2
17	24.7	13.4	18.6	28.0	20.3	12.6	20.9	24.9	9.9	4.2	5.2	7.9	23.7	17.2	12.3	9.6	-	6.2	5.4	15.3	16.6	26.5
18	32.2	17.4	24.1	34.7	19.6	19.7	31.5	32.9	7.1	10.6	9.2	16.6	30.4	25.9	21.4	16.7	6.2	-	7.7	18.2	12.5	28.3
19	28.2	16.6	22.0	27.9	20.2	16.1	27.7	24.1	12.2	10.7	9.4	11.4	23.6	19.2	14.6	10.0	5.4	7.7	-	11.3	20.1	33.2
20	31.2	27.1	30.6	23.6	30.0	22.3	20.1	21.5	21.9	16.9	15.6	8.5	19.3	14.9	10.3	4.9	15.3	18.2	11.3	-	33.1	40.9
21	33.7	18.3	27.5	35.9	16.8	20.0	27.2	30.6	5.7	14.6	17.7	21.2	46.2	41.8	37.3	32.6	16.6	12.5	20.1	33.1	-	19.0
22	28.5	17.3	23.5	34.2	13.7	25.6	27.4	33.0	25.6	24.5	29.0	40.1	32.5	49.4	44.9	40.2	26.5	28.3	33.2	40.9	19.0	-

Table 5. Set of solutions obtained from solving the case study

Efficient solution	ω_1 (\$)	ω_2 (kg)
1	953811.99	1536.24
2	959843.85	1435.12
3	963662.83	1367.24
4	971096.30	1264.36
5	971790.42	1200.81
6	983991.72	1125.75
7	997911.41	1053.25
8	1003876.14	931.09
9	1027044.67	803.25

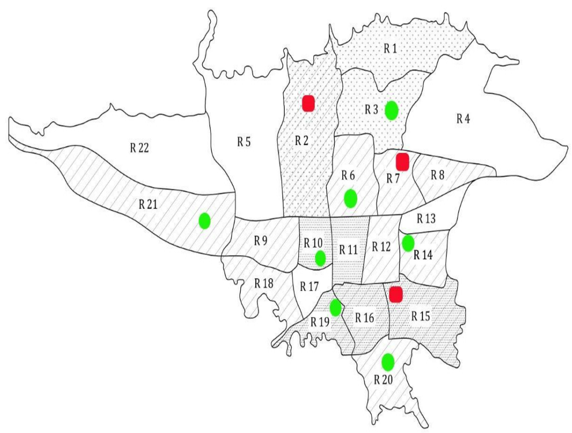

Fig. 4. Location of permanent and temporary aid bases in the first efficient solution.

Table 6. Demand coverage of the 22 districts of Tehran under the case-study disaster scenario

Aid base / public aid flow source	Areas covered
Permanent aid base of region 2	R2 – R5
Permanent aid base of region 7	R7 – R8
Permanent aid base of region 15	R15
Temporary relief base of region 3	R1 – R3 – R4
Temporary relief base of region 6	R2 – R6 – R7
Temporary relief base of region 10	R9 – R10 – R11 – R18
Temporary relief base of region 14	R12 – R13 – R14
Temporary relief base of region 19	R16 – R17 – R19
Temporary relief base of region 20	R20 – R15
Temporary relief base of region 21	R21 – R22
Public aid	R4 – R15

5.1 Key findings and analyses

The numerical results of the case study yield nine efficient solutions that capture the trade-off between total logistics cost and unmet demand under crisis conditions. These solutions provide decision-makers with alternative network configurations reflecting different priority structures. As reported in Table 5, the first efficient solution (Solution 1) is defined as the baseline configuration due to its cost-efficient structure. This solution includes the establishment of three permanent aid bases located in districts 2, 7, and 15, along with seven temporary relief bases located in districts 3, 6, 10, 14, 19, 20, and 21. Under this configuration, the total logistics cost is approximately USD 953,811.99, while the maximum unmet demand reaches about 1,536 kilograms.

A key insight emerging from the analysis is the inherent trade-off between logistics cost and service level across the Pareto frontier. As the number of temporary relief bases increases from Solution 1 to Solution 9, unmet demand decreases by approximately 47.7% relative to the baseline configuration. This improvement is achieved at the expense of higher operational costs due to additional facility deployment and inventory handling. These results highlight the importance of flexible capacity planning in disaster response, where marginal increases in cost can substantially enhance humanitarian performance.

The results further indicate that spatial configuration plays a critical role in system performance. Delivery efficiency is highly sensitive to inter-district distances, and strategic placement of aid bases significantly improves response effectiveness. Compared with the baseline configuration (Solution 1 in Table 5), the most service-oriented solution (Solution 9) achieves approximately a 47–48% reduction in unmet demand, reflecting improved allocation and distribution of perishable relief items. However, this improvement is associated with a higher total logistics cost, highlighting the fundamental trade-off between cost efficiency and service reliability in humanitarian logistics design.

Overall, the findings demonstrate that integrated and flexible logistics planning is essential for effective disaster response. By explicitly incorporating perishability, facility flexibility, and spatial structure, the proposed framework enables decision-makers to manage trade-offs between cost efficiency and humanitarian effectiveness in a transparent, reproducible, and data-consistent manner.

5.2 Sensitivity analysis

This section examines the sensitivity of the two objective values to changes in the uncertainty-control parameters. The analyses use the first efficient solution as the reference configuration. Table 7 reports the results for demand-uncertainty levels α ranging from 0.1 to 0.9. Across this range, both total logistics cost and maximum unmet demand increase as demand uncertainty rises, indicating progressively greater resource requirements and shortage exposure under more adverse demand conditions.

Table 7 shows a monotonic deterioration in both objectives as α increases. Relative to $\alpha = 0.5$, raising α to 0.9 increases total cost from USD 953,811.99 to USD 1,002,478.64 and maximum unmet demand from 1,536.24 kg to 2,134.99 kg. These results demonstrate the importance of strategic flexibility: additional temporary capacity and adaptive allocation can mitigate shortages under more adverse demand conditions, but such measures entail additional operating and transportation costs.

As shown in Fig. 5, increasing demand uncertainty (α) raises both total logistics cost and maximum unmet demand. Increasing α from 0.5 to 0.9 raises total cost by approximately 5.10% and maximum unmet demand by 38.98%. The response is therefore more pronounced for unmet demand than for cost over this interval. From a planning perspective, two implications follow. First, flexible temporary

Table 7. Changes in the values of the objective function of the problem in the uncertainty rates α

α	ω_1 ($)	ω_2 (kg)
0.1	891965.23	1023.48
0.2	911365.18	1128.93
0.3	923548.66	1294.81
0.4	941567.25	1435.58
0.5	953811.99	1536.24
0.6	969846.44	1735.94
0.7	981145.27	1847.62
0.8	993486.37	2098.38
0.9	1002478.64	2134.99

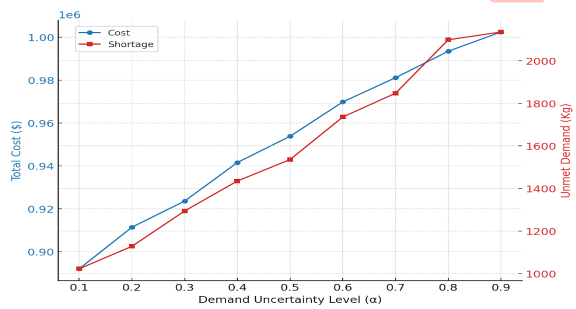

Fig. 5. Sensitivity analysis of demand uncertainty (α) showing its impact on total cost (ω_1) and unmet demand (ω_2)

capacity and adaptive allocation become increasingly important as demand uncertainty grows. Second, the additional service protection obtained from such measures should be evaluated against the associated increase in operating and transportation costs.

Table 8. Changes in the objective function values under different uncertainty levels of β and δ

β , δ	ω_1 ($)	ω_2 (kg)
0.1	896547.61	1223.25
0.2	917384.22	1346.68
0.3	932976.01	1486.28
0.4	953811.99	1536.24
0.5	983894.41	1697.48
0.6	1003524.48	1823.18
0.7	1052185.48	1966.82
0.8	1102463.81	2034.94
0.9	1,128,940.55	2,214.36

The second part of the sensitivity analysis (Table 8) examines the impact of supply-side uncertainty

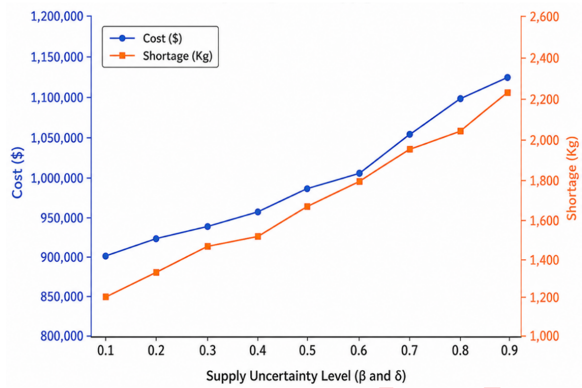

Fig. 6. Sensitivity analysis of supply uncertainty (β and δ) showing its impact on total cost (ω_1) and unmet demand (ω_2)

on logistics performance. As the availability of relief items becomes more uncertain, the model responds by increasing system costs and unmet demand due to reduced effective supply. This highlights the importance of balancing network expansion and budget limitations to ensure reliable disaster response operations.

As shown in Fig. 6, increasing supply uncertainty parameters (β and δ) leads to a consistent increase in both total logistics cost and unmet demand. At low uncertainty levels (0.1–0.3), the system remains relatively stable with moderate variations in performance indicators. However, beyond the moderate uncertainty level (β, $\delta \geq 0.5$), both objective functions increase more rapidly, indicating higher sensitivity of the network to supply disruptions.

Overall, the results confirm that supply-side uncertainty materially affects network performance, reinforcing the value of backup capacity, alternative supply routes, safety-stock policies, and flexible facility deployment. These measures can reduce vulnerability to supply disruptions, but they also increase operating costs; consequently, their use should be calibrated to the decision-maker's budget and service priorities.

5.3 Combined robustness-level analysis

To further investigate the combined effect of uncertainty-control parameters on the behavior of the proposed robust–probabilistic model, a robustness-level analysis was conducted. Unlike the previous sensitivity analyses that separately examine demand uncertainty (α) and supply uncertainty (β and δ), this analysis evaluates the simultaneous variation of α, β, and δ through a unified robustness-control parameter λ. For this purpose, a common robustness-control parameter λ was introduced and defined as:

$$\lambda = \alpha = \beta = \delta. \tag{34}$$

This assumption provides a unified framework for examining how different robustness levels influence the logistics network performance under simultaneous demand and supply uncertainties. For this combined calibration exercise, $\lambda = 0.5$ is used as the reference level. The uncertainty-control settings considered in this analysis are summarized in Table 9.

The corresponding objective values obtained under different robustness-control levels are reported in Table 10. Since the demand and supply uncertainty parameters are increased simultaneously, higher λ values generate more conservative solutions with larger protection against uncertainty.

Table 9. Robustness-control settings used in the calibration analysis

Robustness level	λ	α	β	δ	Interpretation
Very low	0.1	0.1	0.1	0.1	Mild uncertainty
Low	0.2	0.2	0.2	0.2	Low uncertainty
Moderate-low	0.3	0.3	0.3	0.3	Manageable uncertainty
Moderate	0.4	0.4	0.4	0.4	Intermediate uncertainty
Reference	0.5	0.5	0.5	0.5	Reference level for combined calibration
Moderate-high	0.6	0.6	0.6	0.6	Increased uncertainty
High	0.7	0.7	0.7	0.7	Conservative planning
Very high	0.8	0.8	0.8	0.8	Severe uncertainty
Extreme	0.9	0.9	0.9	0.9	Extreme condition

Table 10. Sensitivity of objective values to uncertainty-control parameters

λ	ω_1 ($)	Change in ω_1 vs. base (%)	ω_2 (kg)	Change in ω_2 vs. base (%)
0.1	891965.23	-6.48	1023.48	-33.38
0.2	911365.18	-4.45	1128.93	-26.51
0.3	923548.66	-3.17	1294.81	-15.72
0.4	941567.25	-1.28	1435.58	-6.55
0.5	953811.99	0.00	1536.24	0.00
0.6	969846.44	1.68	1735.94	13.00
0.7	981145.27	2.87	1847.62	20.27
0.8	993486.37	4.16	2098.38	36.59
0.9	1002478.64	5.10	2134.99	38.98

Note: Percentage changes are calculated relative to the base case (λ=0.5) as:$\%\Delta\omega_q = \frac{\omega_q(\lambda)-\omega_q(0.5)}{\omega_q(0.5)} \times 100$, $q = 1,2$. Accordingly, a negative change in ω_2 indicates a reduction in maximum unmet demand relative to the base case and therefore represents an improvement in service performance, whereas a positive value indicates an increase in unmet demand.

The results indicate a clear relationship between the robustness-control level and network performance. As λ increases, both logistics cost and unmet demand increase. This behavior is expected because larger uncertainty levels simultaneously increase effective demand and reduce available supply, forcing the model to operate under more conservative conditions.

Compared with the base case (λ = 0.5), increasing λ to 0.9 leads to a 5.10% increase in total logistics cost and a 38.98% increase in unmet demand. Conversely, reducing λ to 0.1 decreases total cost by 6.48% and unmet demand by 33.38%. Thus, the negative percentage reported for ω_2 at λ¡0.5 should be interpreted as a reduction in unmet demand relative to the base case rather than as a deterioration in performance. These results demonstrate that the proposed robust–probabilistic framework is sensitive to uncertainty-control settings and can effectively capture the trade-off between preparedness and op-

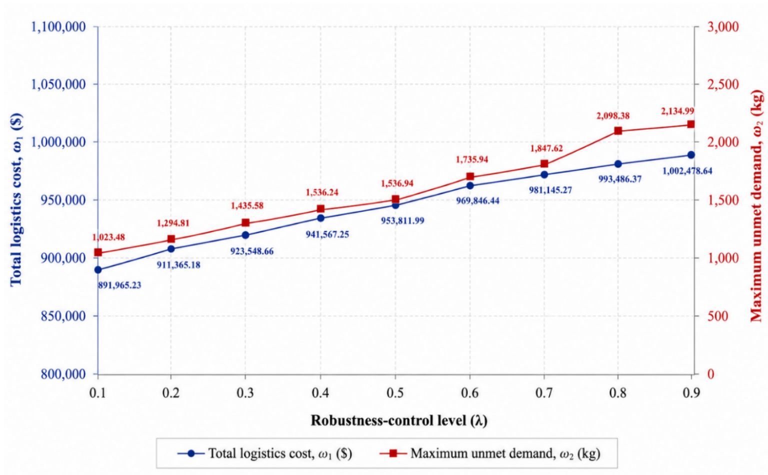

Fig. 7. Sensitivity analysis of total cost (ω_1) and unmet demand (ω_2) under different robustness levels (λ)

erational efficiency. The relationship between robustness level and system performance is illustrated in Fig. 7.

As shown in Fig. 7, both total logistics cost and unmet demand increase monotonically with λ. At low robustness levels (0.1–0.3), the system remains relatively efficient with minor increases in cost and low unmet demand. However, beyond $\lambda = 0.5$, the model becomes increasingly conservative, leading to a sharper rise in both objectives. Specifically, increasing λ from 0.5 to 0.9 results in a 5.10% increase in total logistics cost and a 38.98% increase in unmet demand. Conversely, reducing λ to 0.1 decreases cost by 6.48% and unmet demand by 33.38%. These results confirm that the proposed framework effectively captures the trade-off between preparedness and operational efficiency.

5.4 Performance analysis

The performance analysis summarizes how the two objective values change across the examined uncertainty levels. Consistent with the sensitivity results, increasing uncertainty raises both logistics cost and maximum unmet demand; thus, the network does not remain invariant as conditions become more adverse. The cost increase is comparatively moderate, whereas the shortage measure is more sensitive, particularly at higher uncertainty levels. Fig. 8 visualizes these trends and confirms the need to balance additional preparedness expenditure against the risk of unmet demand.

These results support the use of a mixed permanent–temporary facility structure as a mechanism for adapting to uncertain conditions, while also showing that robustness has a measurable economic and service-level cost.

5.5 Computational performance and scalability analysis

To evaluate the computational applicability of the proposed model beyond the Tehran case study, additional computational experiments were conducted using scaled test instances derived from the baseline

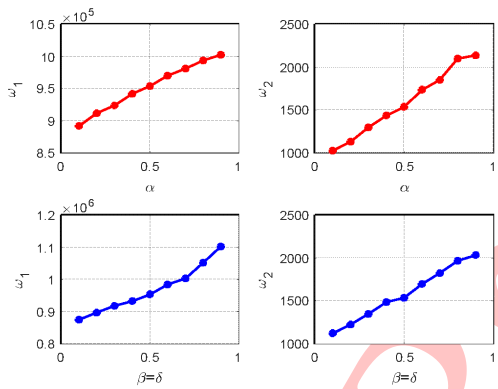

Fig. 8. Trend of changes in objective function values at different uncertainty levels

Tehran network. The purpose of this analysis is to examine the runtime behavior and scalability of the proposed mixed-integer formulation as the size of the crisis logistics network increases.

The model was implemented in the GAMS environment and solved using the CPLEX solver. The enhanced ε-constraint method was used to generate efficient solutions, while each single-objective reformulation was solved by the MIP solver using its branch-and-bound procedure. In the scaled instances, the number of affected areas, candidate permanent aid bases, and candidate temporary aid bases was increased simultaneously, while preserving the main structure of the Tehran case study. Since public aid is modeled as an aggregate aid source in the proposed formulation, one public aid source is considered in all generated instances. The computational results are reported in Table 11. The generated test instances are labeled according to their relative problem size. The prefixes S, M, L, XL, and XXL denote small, medium, large, extra-large, and extra-extra-large instance groups, respectively, while the numerical suffixes (1, 2, and 3) distinguish progressively larger instances within the same group. The "Tehran base" instance represents the original real case-study configuration.

Table 11. Computational performance on scaled test instances

Instance	Class	Nodes	Variables	Constraints	CPU time (sec)	Optimality gap (%)
S1	Small	25	6,790	8,160	4.2	0.00
S2	Small	37	9,020	10,850	9.1	0.00
S3	Small-medium	49	12,140	14,630	18.7	0.00
Tehran base	Real case	67	18,500	22,300	38.5	0.00
M1	Medium	91	30,110	36,330	95.6	0.01
M2	Medium-large	121	49,640	59,920	214.3	0.06
L1	Large	151	74,750	90,250	468.7	0.18
L2	Large	181	105,440	127,320	915.4	0.52
L3	Very large	211	141,710	171,130	1,680.2	1.34
XL1	Extra-large	241	183,560	221,680	2,900.8	2.48
XL2	Extra-large	271	230,990	278,970	3,600.0*	3.95
XL3	Extreme	301	284,000	343,000	3,600.0*	5.60
XXL	Ultra-large	361	406,800	491,300	3,600.0*	8.20

* The predefined time limit of 3,600 seconds was reached; the reported optimality gap is the final relative MIP gap at termination.

The results indicate a clear nonlinear increase in computational effort as the problem size grows. Small and medium instances are solved with negligible optimality gaps and relatively short CPU times. As the network size increases, the residual optimality gap also generally increases. For the largest instances (XL2, XL3, and XXL), the predefined computational time limit of 3,600 seconds was reached before the solver could close the remaining optimality gap. The gap values reported for these instances therefore represent the final relative MIP gaps between the best feasible incumbent solutions and the corresponding best bounds at solver termination. The largest gap is 8.20% for the XXL instance. These results indicate that the proposed formulation remains computationally tractable for small and medium networks, while larger instances can still yield feasible near-optimal solutions within the imposed computational time limit.

Despite this, the obtained solutions remain of high practical quality and provide near-optimal decision support for large-scale humanitarian logistics planning. The results confirm that the proposed model is applicable for small to medium networks and remains solvable with acceptable approximation quality for large-scale disaster scenarios.

5.6 Benchmark comparison analysis

To further validate the effectiveness of the proposed robust–probabilistic framework, a benchmark experiment was designed and evaluated using the same Tehran case-study setting. Three alternative formulations were considered for comparison: a deterministic model, a stochastic-only model, and a robust-only model. The deterministic model uses nominal parameter values and ignores uncertainty. The stochastic-only model considers scenario probabilities but does not include robustness-control parameters. The robust-only model protects the network against adverse demand–supply realizations but does not use probabilistic scenario information. In contrast, the proposed model integrates scenario probabilities with robustness-control parameters, thereby balancing expected performance and protection against adverse conditions.

For consistency, the first efficient solution of the proposed model was used as the reference solution. The comparison was performed based on total logistics cost, maximum unmet demand, and the number of opened permanent and temporary aid bases. The results are summarized in Table **??**.

The benchmark results show that the deterministic model achieves the lowest total cost because it ignores demand and supply deviations. However, this cost advantage is obtained at the expense of substantially higher unmet demand. Compared with the proposed model, the deterministic formulation reduces cost by 11.25%, but increases maximum unmet demand by 74.80%. This indicates that nominal planning may underestimate disaster-response risk.

The stochastic-only model improves upon the deterministic formulation by incorporating scenario probabilities. Nevertheless, because it does not include robustness-control parameters, it remains sensitive to severe demand–supply deviations. Its total cost is 4.31% lower than the proposed model, but its unmet demand is 28.42% higher.

The robust-only model provides the strongest shortage protection, reducing unmet demand by 29.33% compared with the proposed model. However, this improvement is achieved through a considerably higher logistics cost and a larger number of opened aid bases. This confirms that purely robust formulations may lead to overly conservative network designs.

Overall, the proposed robust–probabilistic model provides a balanced alternative. It avoids the under-protection of deterministic and stochastic-only models while preventing the excessive conservatism of the robust-only model. By combining scenario probabilities with controllable robustness parameters, the proposed framework offers a practical trade-off between cost efficiency and humanitarian service reliability.

5.7 Discussion and practical implications

The findings of this study provide several important insights for crisis logistics planning under perishability and uncertainty. The results confirm that the proposed robust–probabilistic framework can support decision-makers in balancing two conflicting objectives: reducing total logistics cost and minimizing maximum unmet demand. The set of efficient solutions reported in Table 5 shows that lower unmet demand can be achieved by expanding temporary response capacity, but this improvement is accompanied by higher logistics and inventory-related costs. Therefore, the model provides a structured decision-support tool for evaluating the trade-off between cost efficiency and humanitarian service reliability.

A key practical implication is the importance of coordinating permanent and temporary aid bases. Permanent aid bases provide stable pre-disaster capacity and ensure that core relief resources are available before the crisis occurs. Temporary aid bases, on the other hand, provide operational flexibility during the response phase and help reduce shortages in highly affected areas. In the Tehran case study, the first efficient solution selects three permanent aid bases and seven temporary aid bases, resulting in a total logistics cost of USD 953,811.99 and a maximum unmet demand of 1,536.24 kg. Moving toward more service-oriented efficient solutions increases the number of temporary bases and reduces unmet demand. Specifically, unmet demand decreases from 1,536.24 kg in solution 1 to 803.25 kg in solution 9, representing an approximate 47.7% reduction. This confirms the managerial value of flexible temporary capacity in disaster response planning.

The sensitivity and robustness-level analyses further show that uncertainty-control parameters have a significant effect on network performance. As uncertainty levels increase, both total logistics cost and unmet demand increase, indicating that crisis logistics networks should not be designed only for nominal or average conditions. From a managerial perspective, this highlights the need for preparedness policies that explicitly account for demand surges and supply reductions. Decision-makers can use the robustness-control parameter λ to evaluate different planning attitudes, ranging from cost-efficient but less protected configurations to more conservative configurations with higher protection against adverse conditions.

The computational scalability results also provide useful implications for practical implementation. The proposed model remains computationally tractable for the Tehran case and for several larger scaled instances, suggesting that the framework can be applied to urban disaster-response networks of larger size. However, for very large national-scale or multi-city disaster scenarios, decomposition algorithms, matheuristics, or customized heuristic approaches may be required to improve computational efficiency and enable faster decision support.

The benchmark comparison provides additional evidence on the practical value of the proposed approach. Compared with the deterministic model, the proposed robust–probabilistic model avoids underestimating disaster-response risk. Compared with the stochastic-only model, it provides additional protection against adverse demand–supply deviations. Compared with the robust-only model, it avoids excessive conservatism and unnecessary cost escalation. Therefore, the proposed framework offers a balanced planning approach by combining scenario probabilities with controllable robustness parameters.

Overall, the results suggest that effective crisis logistics planning requires an integrated approach that jointly considers facility location, temporary response capacity, perishability, public aid flows, and demand–supply uncertainty. For emergency managers and policy-makers, the proposed model can support decisions on where to establish permanent aid bases, where to deploy temporary relief bases, how to allocate perishable relief items, and how to manage public aid flows under uncertain disaster conditions. These capabilities are particularly relevant for large metropolitan areas such as Tehran, where high population density, spatial dispersion, and disaster exposure require coordinated and adaptive logistics planning.

6 Managerial implications

The results of this study provide several managerial insights for the design and operation of crisis logistics systems, particularly in large urban areas where relief demand, supply availability, and the usability of perishable items are highly uncertain. Beyond its analytical contribution, the proposed framework provides practical guidance for policymakers, emergency planners, and humanitarian logistics managers who need to balance preparedness cost, response flexibility, and service reliability.

A central managerial implication concerns the strategic coordination of permanent and temporary aid bases. Permanent aid bases provide stable pre-disaster capacity and ensure that core relief resources are available before a crisis occurs. Temporary aid bases, in contrast, provide operational flexibility during the response phase and help the logistics network adapt to spatially uneven and rapidly changing demand. The Tehran case study shows that the first efficient solution selects three permanent aid bases and seven temporary aid bases, resulting in a total logistics cost of USD 953,811.99 and a maximum unmet demand of 1,536.24 kg. Moving toward more service-oriented efficient solutions increases the number of temporary bases and reduces unmet demand. In particular, unmet demand decreases from 1,536.24 kg in solution 1 to 803.25 kg in solution 9, representing an approximate 47.7% reduction. This highlights the managerial value of flexible temporary capacity in crisis response planning.

The results also emphasize the need to explicitly manage the trade-off between cost efficiency and humanitarian service coverage. The Pareto solutions show that lower unmet demand can be achieved, but only at the expense of higher logistics and inventory-related costs. Therefore, decision-makers should avoid relying solely on cost-minimization policies. Instead, they should evaluate how additional investments in temporary bases, inventory holding, and transportation capacity translate into reduced shortages of perishable relief items. This trade-off is particularly important in disaster environments where small delays or allocation errors may lead to both service failure and product expiration.

The modeling of perishability provides another important operational implication. Relief items with limited shelf lives require time-sensitive inventory and shipment decisions. Managers should therefore prioritize operational mechanisms that reduce delays between supply availability, temporary storage, and final delivery to affected areas. This may include predefining storage locations, improving handling procedures, using appropriate preservation equipment where needed, and ensuring that perishable items are allocated according to their remaining usable life. By explicitly incorporating shelf-life constraints, the proposed model helps managers reduce the risk of allocating expired or unusable items during response operations.

Another key implication relates to the management of public and celebrity donations. In many disaster situations, donated resources can provide valuable additional supply, but unmanaged inflows may create bottlenecks, mismatches, or inefficient allocation. The proposed framework treats public aid as an explicit network flow, allowing donated resources to be directed to permanent bases, temporary bases, or affected areas according to system needs. This suggests that disaster managers should establish clear protocols for receiving, screening, routing, and allocating public aid flows before a crisis occurs.

The sensitivity and robustness-level analyses further show that crisis logistics networks should not be designed only for nominal or average conditions. As the uncertainty-control level increases, both total logistics cost and unmet demand increase. This implies that managers should define acceptable robustness levels based on available budgets, service priorities, and expected disaster severity. The unified robustness-control parameter λ can support this decision by allowing planners to examine different levels of conservatism and evaluate their effects on cost and shortage performance.

The scalability analysis also provides useful managerial insight. The proposed model remains computationally manageable for the real Tehran case and for several larger scaled instances, indicating that it can support urban-level disaster response planning. However, for very large national-scale or multi-city disaster scenarios, exact optimization may become computationally demanding. In such cases, managers and analysts may need to use decomposition algorithms, matheuristics, meta-heuristics, or customized heuristic methods to obtain timely solutions for operational decision-making.

Finally, the benchmark comparison clarifies the practical value of the proposed robust–probabilistic approach. Deterministic planning may underestimate disaster-response risk and result in high unmet demand. Stochastic-only planning improves average-case performance but may remain vulnerable to severe demand–supply deviations. Robust-only planning provides stronger protection but may lead to excessive cost and over-conservative facility decisions. The proposed model offers a balanced alternative by combining scenario probabilities with controllable robustness parameters. This enables decision-makers to avoid both under-protection and unnecessary over-conservatism.

Overall, the managerial insights derived from this study indicate that effective crisis logistics planning requires an integrated and forward-looking approach. Emergency managers should jointly consider permanent facility location, temporary response capacity, perishability constraints, public aid flows, and demand–supply uncertainty. Incorporating these elements into disaster preparedness and response planning can improve the adaptability, reliability, and humanitarian effectiveness of crisis logistics systems under uncertain conditions.

7 Conclusion

This study addressed the problem of locating permanent and temporary aid bases and allocating perishable relief items within a crisis logistics network under demand and supply uncertainty. A bi-objective optimization framework was developed to simultaneously minimize total logistics cost and maximum unmet demand. A two-stage robust–probabilistic approach was employed to integrate scenario probabilities with robustness-control parameters, enabling the model to capture adverse demand increases and supply reductions in a unified structure. By incorporating shelf-life constraints into strategic and tactical decisions, the proposed model provides a realistic representation of perishable relief logistics operations.

The applicability of the proposed framework was demonstrated through a real-world case study of the Tehran metropolitan area. The numerical results generated nine efficient solutions, revealing a clear trade-off between cost efficiency and humanitarian service performance. The first efficient solution was defined as the baseline configuration, while Solution 9 represents the most service-oriented configuration. The baseline solution resulted in a total logistics cost of USD 953,811.99 and a maximum unmet demand of 1,536.24 kg. Moving toward more service-oriented solutions significantly reduced unmet demand to 803.25 kg in Solution 9, corresponding to an approximate 47.7% reduction relative to the baseline, at the expense of higher logistics costs.

The sensitivity and robustness analyses showed that uncertainty-control parameters have a significant impact on network performance. Increasing the robustness level leads to higher logistics costs and greater unmet demand, indicating that crisis logistics networks should not be designed solely under nominal conditions. Specifically, increasing the robustness-control level from 0.5 to 0.9 increases total logistics cost by 5.10% and maximum unmet demand by 38.98%. These results confirm the capability of the proposed framework to support decision-making under different levels of demand–supply uncertainty.

Additional computational experiments confirmed that the proposed formulation remains computationally tractable for the Tehran case and medium-to-large scaled instances, although computational effort increases for extra-large networks. This suggests that while the exact ε-constraint-based approach is effective for moderate-sized problems, decomposition or heuristic methods may be required for very large-scale applications.

The benchmark comparison further validated the advantages of the proposed model. Deterministic models underestimate unmet demand because they ignore uncertainty, while stochastic models improve average performance but remain sensitive to extreme conditions. Robust-only models reduce shortages but lead to overly conservative and costly solutions. In contrast, the proposed robust–probabilistic framework achieves a balanced trade-off by integrating scenario probabilities with controllable robustness parameters.

From a managerial perspective, the findings highlight the importance of combining permanent preparedness capacity with flexible temporary response facilities. Permanent aid bases should be planned based on long-term risk exposure and accessibility, while temporary bases should be deployed dynamically according to disaster severity and spatial demand distribution. The proposed model therefore provides practical decision support for designing adaptive and uncertainty-aware humanitarian logistics systems in metropolitan areas.

Future research can extend this work by integrating additional emergency facilities such as hospitals and fire stations, developing advanced decomposition or hybrid metaheuristic solution methods for large-scale problems, incorporating data-driven demand forecasting and correlated uncertainties, and considering cascading failures and multi-hazard environments. Extending the model to multi-period recovery planning would further enhance its applicability by capturing the transition from emergency response to long-term recovery operations.

Conflicts of Interest

The authors declare no conflict of interest.

References

[1] S. Abbasi, I. Vlachos, S. Rekabi, M. Talooni, *Designing the distribution network of essential items in the critical conditions of earthquakes and COVID-19 simultaneously*, Sustainability **15** (2023) 15900.

[2] A. Aliakbari, A. Rashidi Komijan, R. Tavakkoli-Moghaddam, E. Najafi, *A new robust optimization model for relief logistics planning under uncertainty: a real-case study*, Soft Comput. **26** (2022) 3883–3901.

[3] A. Boostani, F. Jolai, A. Bozorgi-Amiri, *Designing a sustainable humanitarian relief logistics model in pre- and postdisaster management*, Int. J. Sustain. Transp. **15** (2021) 604–620.

[4] A. Diabat, A. Jabbarzadeh, A. Khosrojerdi, *A perishable product supply chain network design problem with reliability and disruption considerations*, Int. J. Prod. Econ. **212** (2019) 125–138.

[5] S. Khalilpourazari, A. Arshadi Khamseh, *Bi-objective emergency blood supply chain network design in earthquake considering earthquake magnitude: a comprehensive study with real-world application*, Ann. Oper. Res. **283** (2019) 355–393.

[6] Z. Mahtab, A. Azeem, S.M. Ali, S.K. Paul, A.M. Fathollahi-Fard, *Multi-objective robust-stochastic optimisation of relief goods distribution under uncertainty: a real-life case study*, Int. J. Syst. Sci. Oper. Logist. **9** (2022) 241–262.

[7] M. Modiri, M. Eskandari, S. Hasanzadeh, *Multi-objective modeling of relief items distribution network design problem in disaster relief logistics considering transportation system and CO_2 emission*, Sci. Iran. **32(4)** (2025) 1–21.

[8] M.K. Nayeem, G.M. Lee, *Robust design of relief distribution networks considering uncertainty*, Sustainability **13** (2021) 9281.

[9] S. Nodoust, M.S. Pishvaee, S.M. Seyedhosseini, *A robust possibilistic programming model for disaster relief routing under information and communication technology*, Int. J. Supply Oper. Manag. **10** (2023) 38–56.

[10] R. Rajabi, E. Shadkam, S.M. Khalili, *Design and optimization of a pharmaceutical supply chain network under COVID-19 pandemic disruption*, Sustain. Oper. Comput. **5** (2024) 102–111.

[11] A.S. Safaei, S. Farsad, M.M. Paydar, *Emergency logistics planning under supply risk and demand uncertainty*, Oper. Res. **20** (2020) 1437–1460.

[12] K. Sarmadi, M. Amiri-Aref, *A distributionally robust optimisation with joint chance constraints approach for location-routing problem in urban search and rescue operations*, Comput. Oper. Res. **180** (2025) 107051.

[13] H. Seraji, R. Tavakkoli-Moghaddam, S. Asian, H. Kaur, *An integrative location-allocation model for humanitarian logistics with distributive injustice and dissatisfaction under uncertainty*, Ann. Oper. Res. **319** (2022) 211–257.

[14] E. Shadkam, M. Cheraghchi, *Prioritization of earthquake relief using a hybrid two-phase approach*, J. Appl. Res. Ind. Eng. **9** (2022) 493–506.

[15] E. Shadkam, M. Parvizi, R. Rajabi, *The study of multi-objective supplier selection problem by a novel hybrid method: COA/ε-constraint*, Int. J. Res. Ind. Eng. **10** (2021) 223–237.

[16] B. Vahdani, D. Veysmoradi, F. Noori, F. Mansour, *Two-stage multi-objective location-routing-inventory model for humanitarian logistics network design under uncertainty*, Int. J. Disaster Risk Reduct. **27** (2018) 290–306.

[17] W. Wang, K. Yang, L. Yang, Z. Gao, *Distributionally robust chance-constrained programming for multi-period emergency resource allocation and vehicle routing in disaster response operations*, Omega **120** (2023) 102915.

[18] Z. Wang, Y. Liu, W. Li, *A globalized robust optimization method for sustainable humanitarian relief network design with uncertain scenario probabilities*, Sustain. Cities Soc. **97** (2023) 104729.

[19] G. Zhang, N. Jia, N. Zhu, L. He, Y. Adulyasak, *Humanitarian transportation network design via two-stage distributionally robust optimization*, Transp. Res. Part B **176** (2023) 102805.

[20] T. Zhang, S. Wang, X. Xin, *Humanitarian relief logistics network design considering facility location, inventory pre-positioning and evacuation planning: a two-stage distributionally robust optimization approach*, Comput. Oper. Res. **189** (2026) 107390.

[21] X. Zhang, D. Chen, *Prepositioning network design for humanitarian relief purposes under correlated demand uncertainty*, Comput. Ind. Eng. **182** (2023) 109365.

[22] M. Ziaee, M. Imanparast, V. Khodabakhshi, *Multi-agent single machine scheduling problem with transportation constraints*, J. Math. Model. **10(3)** (2022) 367–385.